

Republic of Iraq

Ministry of Higher Education and Scientific Research

University of Babylon / College of Science

Department of Physics



Study the Effect of Weather Temperature on the Spectra of Gamma Rays for the Scintillation Detector NaI(Tl)

A thesis

Submitted to the Council of the College of Science University of
Babylon in Partial Fulfillment of the Requirements for the degree
of Master of Science in Physics

By

Abbas Hassan Abedullah Zaeiri

Supervised by

Prof. Dr. Khalid H. Hatif. Al-Attiyah

2021 A.D.

1443 A.H.

بِسْمِ اللّٰهِ الرَّحْمٰنِ الرَّحِیْمِ

﴿ یرفع اللّٰه الذین امنوا منکم والذین اوتوا العلم درجات

والله بما تعملون خبیر ﴾

صدق الله العظیم

سورة المجادلة ﴿ ١١ ﴾

Acknowledgments

Thanks Allah for helping me to complete this study...

*I would like to express my gratitude and sincere thanks to my supervisor **Prof. Dr. Khalid. H. Hatif** for his encouragement over the period of the research...*

My thanks to professors, teachers and the members in Babylon University / College of Science / Physics Department...

My thanks are also extended to all my colleagues in the department...

It is also of my pleasure to acknowledge the advice and assistance that I have received from all other people

Abbas

Dedication

To....

My Mother

To....

My Family

To....

My Wife

To....

Every one help me

Abbas

Summary

The effect of the weather temperature on the energy spectrum by the scintillation detector NaI(Tl) has been studied in this work. Several standard radioactive sources have been used, including (Cs-137), (Na-22) and (Co-60), a heat source was used to control the temperature. Used also thermometers on right and left side from the detector to measure the appropriate temperature. used also a container with a heat-insulating cover to containing all these parts that were used in the experimental side to maintain the temperature constant to obtain on the best results.

It was found that the photo peak position (centroid) decreases in the area of the spectrum with the increase in temperature (inverse proportionality) in the spectra of all the elements that were used, and it is the clearest behavior obtained, as for the all the results of area, most of the time their effect increases with temperature, and they have no clear behavior, also the net and gross for total area ,photo peak1 and photo peak2 have same behavior.

Through the results obtained, it was found that the position of the photo peak of the product spectrum is affected by temperature, whenever the temperature increases, the resulting spectrum from the scintillation detector is compressed and the position photo peak change to the lower channel levels so the temperature must be constant during use.

Contents

<i>No.</i>	<i>Subject</i>	<i>Page No.</i>
	Contents	II
	List of Figures	IV
	List of Tables	IX
	List of abbreviations and symbols	X
<i>Chapter One</i> <i>General Introduction</i>		
1.1	Introduction	1
1.2	Previous Studies	2
1.3	Aim of the study	8
<i>Chapter Two</i> <i>Theoretical part</i>		
2.1	Introduction	9
2.2	Gamma ray	9
2.3	Gamma source	9

<i>No.</i>	<i>Subject</i>	<i>Page No.</i>
2.4	Interactions Gamma rays with matter	10
2.4.1	The Photoelectric Effect	10
2.4.2	Compton scattering	10
2.4.3	Pair Production	10
2.5	Scintillation detector	11
2.5.1	NaI(Tl) Detector	11
2.5.1.1	Effect temperature on the NaI (Tl) crystal	11
2.5.1.2	Effect temperature on the photomultiplier	12
2.6	NaI(Tl) detector uses	13
2.6.1	Nuclear physics	13
2.6.2	Environment field	13
2.6.3	Nuclear medicine	14

<i>No.</i>	<i>Subject</i>	<i>Page No.</i>
2.6.4	Explosives detection field	14
<i>Chapter Three</i> <i>Practical part</i>		
3.1	Introduction	15
3.2	Electronic counting and analysis system	15
3.2.1	Preamplifier	15
3.2.2	Main amplifier	15
3.2.3	High Voltage power supply	15
3.2.4	Multi-Channel Analyzer (MCA)	15
3.3	Radioactive Sources	17
3.4	Geometric Configuration	21
<i>Chapter Four</i> <i>Results, Discussion, Conclusions and Suggestions</i>		
4.1	Cs-137	22

<i>No.</i>	<i>Subject</i>	<i>Page No.</i>
4.1.1	Total spectrum area for Cs-137	24
4.1.2	Photo peak at (0.662 MeV)	26
4.2	Na-22	31
4.2.1	Total Area	32
4.2.2	Photo peak1 at (0.511MeV)	34
4.2.3	Photo peak2 at (1.276 MeV)	39
4.3	Co-60	45
4.3.1	Total Area	46
4.3.2	Photo Peak1 at (1.173 MeV)	48
4.3.3	Photo Peak2 at (1.332MeV)	53
4.4	Conclusions	59
4.5	Future Works	60
	References	61

List of Figures

No.	Title of Figure	Page No.
2.1	NaI(Tl) detector	11
2.2	Relative pulse and temperature.	12
3.1	The Block diagram of the counting system	16
3.2	Counting and analysis system	16
3.3	Cs – 137 spectrum	18
3.4	Na- 22 spectrum	19
3.5	Co – 60 spectrum	20
3.6	Geometric configuration	21
4.1	Distribution Net count with change temperature for Cs-137 total area.	24
4.2	Distribution Gross count with change temperature for Cs-137 total area.	25
4.3	Distribution Net count with change temperature for Cs-137 photo peak.	26
4.4	Distribution Gross count with change temperature for Cs-137 photo peak.	27

<i>No.</i>	<i>Title of Figure</i>	<i>Page No.</i>
4.5	Distribution FWHM with change temperature for (Cs-137) photo peak.	28
4.6	Distribution position photo peak (centroid) with change temperature for (Cs-137) photo peak.	29
4.7	Distribution E.R with change temperature for (Cs-137) photo peak.	30
4.8	Distribution Net with change temperature for (Na-22) for total area.	32
4.9	Distribution Gross with change temperature for (Na-22) for total area.	33
4.10	Distribution Net with change temperature for (Na-22) photo peak1.	34
4.11	Distribution Gross with change temperature for (Na-22) photo peak1.	35
4.12	Distribution the FWHM with change temperature for (Na-22) photo peak1.	36
4.13	Distribution centroid with change temperature for (Na-22) photo peak1.	37
4.14	Distribution E.R with change temperature for (Na-22) photo peak1.	38
4.15	Distribution Net with change temperature for (Na-22) photo peak2.	40
4.16	Distribution Gross with change temperature for (Na-22) photo peak2.	41

No.	<i>Title of Figure</i>	<i>Page No.</i>
4.17	Distribution FWHM with change temperature for(Na-22) photo peak2.	42
4.18	Distribution centroid with change temperature for(Na-22) photo peak2.	43
4.19	Distribution E.R with change temperature for(Na-22) photo peak2.	44
4.20	Distribution Net with change temperature for(Co-60) Total area.	45
4.21	Distribution Gross with change temperature for (Co-60) Total area.	47
4.22	Distribution Net with change temperature for (Co-60) in the photo peak1.	48
4.23	Distribution Gross with change temperature for (Co-60) Total area.	49
4.24	Distribution FWHM with change temperature for (Co-60) Total area.	50
4.25	Distribution position photo peak 1 with change temperature for (Co-60) photo peak1.	51
4.26	Distribution E.R with change temperature for (Co-60) photo peak1.	52
4.27	Distribution Net with change temperature for (Co-60) photo peak2.	54
4.28	Distribution Gross with change temperature for (Co-60) photo peak2.	55

<i>No.</i>	<i>Title of Figure</i>	<i>Page No.</i>
4.29	Distribution FWHM with change temperature for (Co-60) photo peak2.	56
4.30	Distribution centroid with change temperature for (Co-60) photo peak2.	57

List of Tables

<i>No.</i>	<i>Title</i>	<i>Page No.</i>
2.1	Radioactive sources was use in experimental part	17
4.1	The results of work for Cs-137.	23
4.2	Results of the effect of temperature on the total area and first photo peak of Na-22.	40
4.3	Results of the effect of temperature on the second photo peak of Na-22.	39
4.4	Results of the effect of temperature on the second photo peak of Co-60.	45
4.5	Results of the effect of temperature on the second photo peak of Co-60.	53

List of abbreviations and symbols

<i>Symbol</i>	<i>Description</i>
Net	The net area of the photo peak without entering the area of the continuation area in the calculation
Gross	The area of the photo peak minus the net area
FWHM	Full Width High Maximum
Centroid	photo peak Position (centroid)
H.V	High Voltages
MCA	Multi –Channel Analyzer
T.A	Total Area
N.T.A	Net Total Area
G.T.A	Gross Total Area
P.N.A	Photo Peak Area
P.G.A	Photo peak Gross Area
UCS-30	Universal Computer Spectrum

<i>Symbol</i>	<i>Description</i>
T	Kinetic energy
E_{γ}	Energy of the photon
BE	Binding energy of the electron
$E_{\gamma'}$	The energy of the photon scattered
$T_{e^{-}}$	Energy of the electron
$T_{e^{+}}$	Energy of the positron
UCS	Universal Computer Spectrometer
E.R	Energy Resolution

Chapter One

General

Introduction

1.1 Introduction

Radiation is energy emitted as a particles or electromagnetic waves, and the radiation is of two types (ionizing, non-ionizing) radiation . Non-ionizing radiation has a little amount of energy, and this radiation has no ability to cause ionization in the cells of the human body (no ionization of the atoms of the medium) [1]. Ionizing radiation has high energy and has the ability to cause ionization in the cells the body(ionization of the atoms of the medium) , such as Alpha and Beta particles, X-ray and gamma rays [2].

As a result of using the detector in different environmental conditions , and as is well known in Iraq , temperature rise in summer to high levels exceeding 45°C and decrease in winter ,as well as the variation during same day, so this major reason for studying this effect on energy spectra by using NaI(Tl) detector. In this research studied the effect of weather temperature on the spectra of the gamma rays for the scintillation detector NaI(Tl). There are a multiple uses of this type of detector for the detection of gamma rays. NaI(Tl) use in different environmental fields and at variable temperatures to known if there is an effect of this continuous change of temperature on the detector work. Scintillation detector use for the detection the radiation resulting from decay the radioactive nuclei such as (potassium 40, uranium and thorium). Radiation detection is one of important role in many applications therefore the scintillation detector use in a wide range of fields for the detection of nuclear rays including health physics and in, environment field and in the high energy physics experiments [3].

This detector also use in one of its most important applications in the field of nuclear medicine is cameras fluorescent gamma consisting of a large crystal of sodium iodide NaI(Tl) and a large number of photomultipliers [4].One of important methods in the field of scientific physical, environmental and biological research is the use of radioactive element [5]. The gamma ray is an electromagnetic ray that has no charge, so it is no affected by the electric or magnetic field. Gamma rays are

emitted from natural and industrial radioactive source in the form of photons .It is characterized by its high penetration [6]. Gamma ray emitted from the isotopes is one of approach which its loss the excitation nuclide from the excess energy to converted these nuclide from high energy level to low energy level that's known radiation decay [7]. Detectors have evolved with development of nuclear physics .These detectors detect radiation by measuring its energy and depend on the interaction between the nuclear radiation and detector material. The flash detectors are characterized by high absorption [1]. The continuous change in source activity from moment to other due the random nature of radioactive decay also there are fluctuate in in the rate of decay that's return to the half- life radionuclide[8].

1.2 Previous Studies

In 2004 P.L. Reeder and D.C. Stromswold [9] studied changes in the pulse by using sodium iodide activated with thallium NaI(Tl) detector, and the results of their study can be measure the changes in the pulse height and the clarity of the photo peak as a function of temperature within the range (- 50 to +60).

In 2005 A. Mowlavi *et al.* [10] study the change in the internal efficiency of the sodium iodide activated by thallium NaI(Tl) versus the "distance between the radioactive source and the detector" the different energies of the rays were calculated using the MCNP program (Monte Carlo Neutral Particle). It was found through the study that the internal efficiency of the detector does not depend only on the energy of the photons , but also depends on the geometric arrangement of the source and the detector, and the change in the internal efficiency of the detector can be analyzed by the average path length of the photons in the detector and the average length of the interaction on the photons.

In 2006 M. Nikl [11] was study the state of x-ray interaction with solid materials was explained, and the performance of these materials by presenting a description of the luminescent materials used and configurations of the NaI(Tl)

detector. Extended description of the materials currently in use or under intense study is given. Scintillation detector configurations are further briefly overviewed and selected applications are mentioned in more detail to provide an illustration.

In 2007 N. Mercier and C. Falgueres [12] was study the use of commonly radioactive detectors for the purpose of determining gamma dose rates such as sodium iodide activated with thallium NaI(Tl). These systems record the gamma spectrum, so the dose rate is measured from the recorded count rates for certain number of "windows" . Through this technique , a small portion of the spectrum is used. It is also possible to use the threshold technique as an alternative approach with the same technology (the system), which has been in common use for more than 25 years.

In 2008 A. D. Sabharwal *et al.* [13] studied the response function of the detector NaI(Tl) , as it including the study of the effect of the thickness of the target on the distribution of the intensity of the gamma photons each time by using aluminum as a target material. Through these study, it was found that NaI(Tl) detectors have a high ability to detect these photons.

In 2009 K.D. Ianakiev *et al.* [14] was study a familiar fact that the total measured light yield of NaI(Tl) detectors is a nonlinear function of temperature. Present new experimental data for the temperature behavior of doped NaI(Tl) scintillators that instead shows a linear dependence of the light output over a wide temperature range—including that for outdoor applications. The redistribution of the intensities between the two processes is temperature dependent; the second (slow) decay component is negligible at room temperatures, but by -20°C , it contributes up to 40% of the total light and has a duration of several microseconds. found effect this new understanding of the light output has on the pulse-height analysis instrumentation.

In 2010 study Y. Zhang *et al.* [15] improved a method of light control and directly monitoring the internal temperature of the scintillation detector NaI(Tl). This method is used to measure width pulse its depending on temperature with Pulse Shape Analyzer (PSA). The study showed that the relation width pulse with temperature is a polynomial relation of the third degree.

In 2011 W.S. Choong *et al.* [16] studied first measurement of the decay times of NaI(Tl) as a function of the deposited electron energy. It has been suggested that the decay curve depends on the ionization density, which is correlated with the electron energy deposit in the scintillator. The ionization creates excitation states, which can decay radioactively and non- radioactively through a number of collecting processes. As a result, the rate at which the excitation decays depends on the ionization density. While a slight dependence of the decay time constants on the electron energy deposit is observed, the results are not statistically significant

In 2012 C. Sailer *et al.* [17] was study The scintillation light output of a pure and a Thallium doped Sodium Iodide NaI(Tl) crystal under irradiation with 5.486MeV alpha -particles has been measured over a temperature range from 1.7K to 300K. Estimates of the decay time constant at three selected temperatures are given. For pure NaI(Tl) an increase in light yield towards low temperatures could be confirmed and measured at higher precision. For NaI(Tl) below 60K an increase in light output has been found.

In same year M.A. Mohamed [18] studied calibrating the NaI(Tl) scintillation detectors (2x2and 3x3) inch and calculating the energy efficiency of the peak energy of standard sources at different distances on the axis of the detector which uses analytical principle of the effective solid angle ratio. It is found this principle is based on mathematical method presented from other researchers.

In 2013 B. Oto *et al.* [19] studied the use of NaI(Tl) scintillation detector to study the radiation that protects the properties of concrete material using radioactive sources Ba-133 and at different rates (variable rates) by using (80.99 and 303) keV energies. The results of this study were in attenuating gamma rays, so the pure concrete is more effective than ordinary concrete.

In the same year A. Simon *et al.* [20] studied the measurements of cross-sections in the nuclear reaction, which has to do with astrophysical process in the modernization (development) of new experimental process that allow the investigation of cross-sections in most cases. This detector is a barrel a new summing NaI(Tl) detector (SuN) its read by 24 photomultiplier.

In 2014 K. U. Kiran *et al.* [21] studied based on the energy of the thickness of saturation with energies (59.54,123,279,511,662,1115 and 1250) keV. It was found that with increase in the thickness of the target material, the number of photons suffer from multiple scattering increases to reach a certain thickness that becomes saturated called (saturation thickness), and this thickness increases with increasing falling photon gamma energy.

In same year S. Takeuchi *et al.* [22] study A NaI(Tl) detector array called DALI2 (Detector Array for Low Intensity radiation 2) has been constructed for in-beam γ -ray spectroscopy experiments with fast radioactive isotope (RI) beams. It consists of 186 NaI(Tl) scintillators covering polar angles from $\sim 15^\circ$ to $\sim 160^\circ$ with an average angular resolution of 6° in full width at half maximum. Good angular resolution enables Doppler-shift corrections that result.

In 2015 Y. Liu *et al.* [23] studied develop in situ NaI(Tl) detector for radioactivity measurement in the marine environment, the Monte Carlo N-Particle (MCNP) Transport Code was utilized to simulate the measurement of NaI(Tl) detector immersed, taking into account the material and geometry of the detector, and the interactions between the photons with the atoms. The simulation results of the

marine detection efficiency and distance were deduced and analyzed. In order to test their reliability, the field measurement was made at open sea and the experimental value of the marine detection efficiency was deduced and seems to be in good agreement with the simulated one. The simulation method and results in the paper can be used for the better design and quantitative calculation of in situ NaI(Tl) detector for radioactivity measurement in the marine environment.

In 2016 P. Mitra *et al.* [24] studied spectra of gamma-ray spectrometer a method was standard to restore a shifted different pulse height spectrum (a gamma – ray spectrometer based on a recorded flash at standard temperature), to position spectrum at the reference temperature .This method was developed and used at different temperature and was used to receive the measured gamma spectra .To calculate converted between the energy and shift spectrum recovery develop a computer program to calculate this .Its approach a depended on the spectrum obtained in the measurement temperature represents the same statistical distribution of other temperature , but with different scales.

In 2017 De. Souza *et al.* [25] was study using NaI (Tl) detectors the first search for a dark matter (annual modulation signal) in the Southern Hemisphere, performed by the DM-Ice17 experiment. Nuclear recoils from dark matter interactions. DM-Ice17, the first step in the DM-Ice17 experimental program, consists of 17 kg of NaI (Tl) located at the South Pole.

In 2018 L. E. Robalino *et al.* [26] study by Monte Carlo approach for materials detection system made up with a NaI (Tl) gamma detectors and DD neutron generators. These approach is used to analyze the response of the system to different materials (different samples) of explosive, for example NH_4NO_3 . The generator (D-D) can produce fast neutrons that greatly contribute to the detection of

the explosives in the field national security. This method (procedure) allows to determine the type of substance and its chemical composition.

In 2020 M. K. Bakhshayesh [27] studied using the resulting spectrum from low-resolution devices to develop a technique for creating high-resolution detectors such as NaI(Tl), higher energy spectrum. Due to the not found a clear model (mathematical model) between these types of organic and inorganic detectors, that is model-free methods. The result from these study it is found relation between inorganic spectrum pulse organic flash (organic scintillation).

In 2021 S. A. Rasha [28] studied the review of the distribution of radionuclides using spectral distribution of gamma rays in different area of soil in Iraq. The concentration of radionuclide activity in water, air, and rocks were measured for the purposes of monitoring these risks resulting from the effects radiation. It was concluded that the concentrations are less than the global average with the exception of some regions.

In same year L.J. Bignell *et al.* [29] studied measured the quenching factor of the nuclear recoil from the NaI(Tl) detector which is determined by the spectrum. They measured the nuclear reaction in sodium NaI(Tl) crystals after dispersion. The light produce from this recoil process can be reduced for electron by cooling factor, which is very important in dark matter research for the purpose of searching for nuclear scattering reactions.

In same year P. A. Amado *et al.* [30] was study theoretical approach for determining the total peak by calculating the efficiency and calculating total area which is widely used in gamma ray spectroscopy, using five different detector two NaI(Tl) and three HPGe detectors with different crystal sizes and energies . The result was compatibility these theory with Monte Carlo simulations and available experimental data.

1.3 Aim of the study

The purpose of the research is to show the effect of temperature change on the scintillation detector of gamma ray spectrum and to show whether it is possible to use this detector in different environments with different temperatures.

Chapter Two

Theoretical part

2.1 Introduction

Radiation is a part of the natural environment[31]. The Non Ionization Radiation (NIR) does not enough energy to produce ions, it has less energy than ionizing radiation such as visible light ,microwave ,infrared IR, radio wave and ultraviolet UV. Ionizing Radiation (IR) it has great amount of energy it can be occurrence ionization in human cell [32]. It capable of "take off electrons out their orbits around atoms .Ionizing radiation includes the radiation that comes from both natural and man-made radioactive materials". Example of ionization radiation such as Alpha and Beta particles, X-ray and Gamma ray [33].

Background radiation is generated principally by three sources radiation from radioactive elements in our bodies, cosmic radiation and terrestrial radiation. The terrestrial radiation different over the earth due in the earth's surface the differences in the amount of the naturally occurring elements and the building materials maybe merge naturally occurring radioactive materials. The Cosmic radiation levels varietal with elevation. The radiation background can be calculate in any place by the detector without using any radiation source [34].

2.2 Gamma ray

It is an electromagnetic ray that does not have a charge, so it is not deflected by the electric and magnetic field. The gamma ray emits from natural and industrial sources in the form photon [35]. Gamma rays are ray of short wavelength that are emitted in many ways, which results daughter nucleus with a short half-life where the daughter nucleus return to a stable state through the emission of gamma rays with an energy equal to the energy difference between the two planes.

2.3 Gamma source

In radioactive decay, the gamma ray can be product from an unstable (excited) nucleus emitting an excess energy as an electromagnetic wave when its returns to a ground state. The gamma rays also produced with other products such as α or β particles. Gamma rays has a frequency is above 10^{19} Hz. The different between

gamma ray and X-rays although both of them have the range of frequencies overlapping. The X-rays are emitted by electrons while a gamma rays comes from the nuclei of radioactive atoms [36].

2.4 Interactions Gamma rays with matter.

2.4.1 The Photoelectric Effect

The photoelectric between photon and bound atomic electron, as a result of the interaction, the photon disappear and one of atomic electron ejected as a free electron, called the photoelectron. The kinetic energy(T) of electron as equation (2.1) [1].

$$T = E_{\gamma} - BE \quad (2.1)$$

Where E_{γ} energy of photon and BE binding energy of the electron

2.4.2 Compton scattering

An interaction occurs between a photon and external electron, and a partial absorption of energy to the incident photon occurs. The result a photon and electron of the interaction. The remaining energy gives a scattered photon with less energy, so the law of conservation of energy is as in equation (2.2).

$$T = E_{\gamma} - E_{\gamma'} \quad (2.2)$$

Where $E_{\gamma'}$ energy of photon scattering

2.4.3 Pair Production

Is interaction between a photon and nucleus. The photon disappear and an electron – positron appear. The conservation for kinetic energy to the electron – positron is given by equation (2.3)[1].

$$T_{e^-} + T_{e^+} = E_{\gamma} - 1.022 \text{ MeV} \quad (2.3)$$

Where T_{e^-} kinetic energy to the electron and T_{e^+} kinetic energy to the positron

2.5 Scintillation detector is an instrument for detecting and measuring ionizing radiation by using the excitation effect of incident radiation on a scintillating material, and the resultant light pulse, as example of this type of detectors is NaI(Tl).

2.5.1 NaI(Tl) Detector

This detector including two mains parts are scintillation materials and photomultiplier tube .The scintillator material is characterized by the production of photons in the material after it absorbs the gamma rays that as shown in figure(2.1). The thallium addition to the material as impurities to enhance from scintillation process , to causing the excitation of its atoms, and to get rid of the excess energy, thallium atoms are radiated [37].

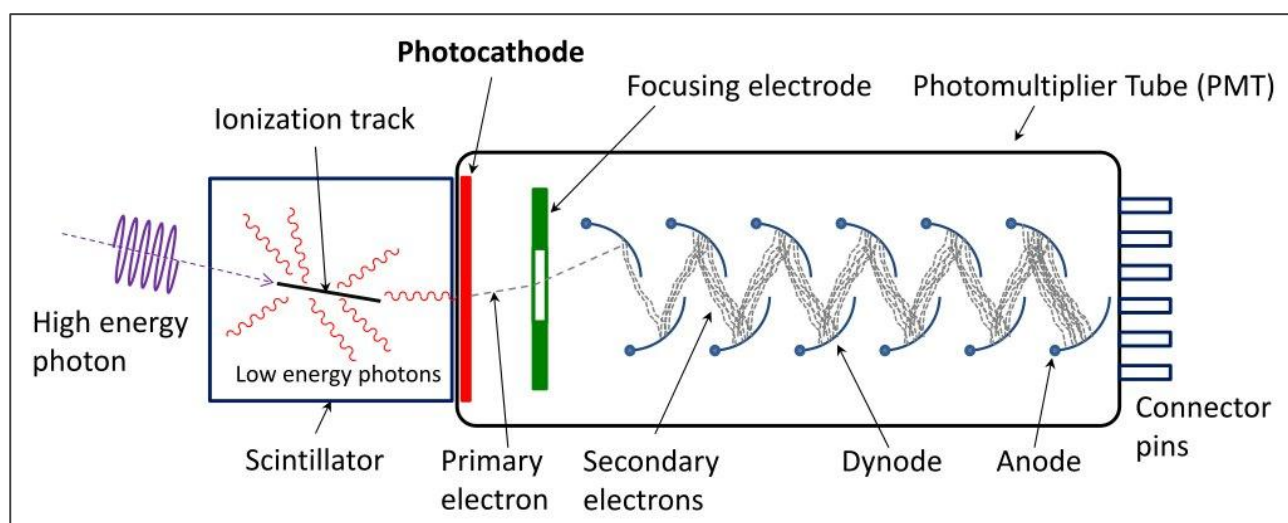


Figure (2.1) NaI(Tl) detector .[36]

2.5.1.1 Effect temperature on the NaI (Tl) crystal

The increase in temperature affects the crystal, generating secondary levels between the "conduction band and the valance band", and the electrons gain vibration energy that enable them to move from the valance band to the conduction band [38]. The light yield in NaI (Tl) as a function of temperature .That is meaning drop off in scintillation yield when get temperature increasing. The temperature dependence of the light product from NaI (Tl) crystals that is shown in figure (2.2). The various in

the behavior between these crystals is probable return to the different in surface reflectively. The temperature also as a function to the time decay (time decay dependence on the temperature when the temperature increasing the time decay decrease [39,40]. The crystal to prevent scattered gamma rays must be thin in "order from being absorbed and to prevent their sustaining additional Compton scatterings before being absorbed [41]. NaI(Tl) scintillation crystal in an Anger camera after the temperature in the imaging room had dropped, which caused the crystal to crack. Prevention of crystal damage due to temperature fluctuations requires that there be an automatic temperature control in constant operation [42].

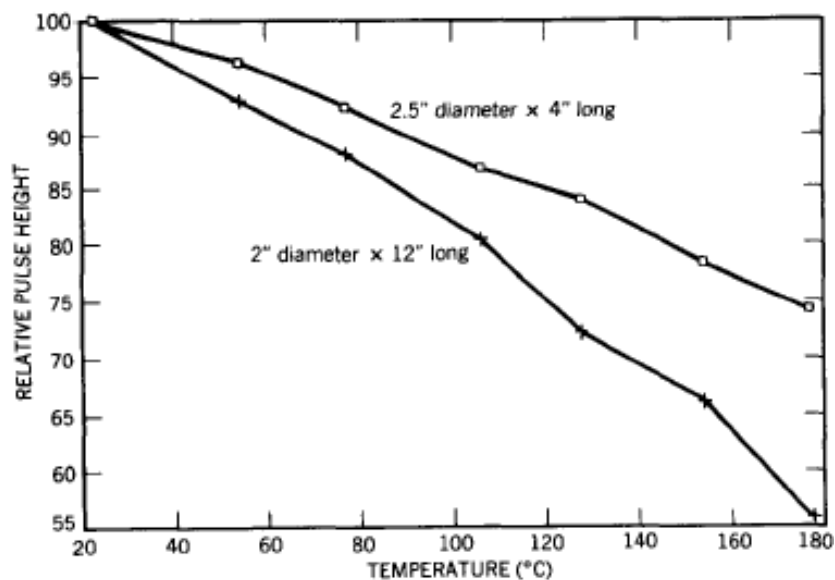


Figure (2.2) Relative pulse and temperature. [1]

2.5.1.2 Effect temperature on the photomultiplier

In the photomultiplier, photons are absorbed and an electron is released, and there is a direct relation between the intensity of the incident light and the current produced by the photomultiplier. The photomultiplier has a very fast response to the light, so it is used to measure the intensity of light sources. A photomultiplier is a development of a photocell that use transistor to amplify small.

In the absence of incident light and potential difference applied to the photomultiplier dynodes, a current called the dark current is generated .One of most

important factor that affected the production of the dark current is the temperature, and the main part of the dark current it is due to the ionic thermal electron that are emitted from the sensitive coating. The best way to reduce the dark current in photomultiplier is to reduce the temperature. The dynode make to doubling an electrons from photocathode in the photomultiplier[42] .

2.6 NaI(Tl) detector uses

There are many fields for the scintillation detector is used such as radiation nuclear physics, environmental field, medicine(nuclear medicine),in field detonations detection ,in apparatus for monitoring of radionuclides, , high energy physics and field of space, etc.

2.6.1 Nuclear physics

In the field of nuclear physics, fluorescence detectors are the common and widely used as a spectroscopy γ - ray detector .The scintillation detector has been widely used for at least 50 year in this field. currently there are many detectors that have been developed in this field [41].

2.6.2 Environment field

One of these methods for determining natural activities, these method is widely used in proposing radionuclides in environmental samples using scintillation (fluorescence) spectroscopy and is based on analyzing the spectra of samples based on the spectral components of a group of separate radionuclides with the help of standard sources. This method has been used without liquid to cool the detector (nitrogen) [42]. In the field of the aquatic environment, NaI(Tl) was used instead of the germanium detector to directly deal with the flow of radioactive materials into water resources because this detector has a large linear response, High density, and appropriate manufacturing technology [43]. It was found that the use of sodium iodide detector with (SiPM) is more efficient in aquatic environment (measurements

for radionuclide detection in aquatic environment) due to the low sensitivity to magnetism, the ability to amplification production, and the low bias process [45,46].

2.6.3 Nuclear medicine

This field is considered one of the most important field in which the scintillation detector NaI(Tl) is widely used. In nuclear medicine there are many types of detector used to get on best quality image and get on accurate diagnosis in nuclear medicine [46]. The studies focus on many properties of such as energy resolution ,density and decay time this properties it is more factors effecting on the image quality .Nuclear medicine imaging entire in the context anatomy, molecular level to diagnosis of disease, physiology and determination of drugs distribution in body [47-49]. A scintillation crystal with short decay time, high density, high luminous efficiency, good spectral match to photo detectors. NaI(Tl) is parts of Gamma camera imaging and NaI(Tl) is the oldest and most common crystal in 1948 was introduced [50]. NaI(Tl) which it common crystal for use imagining equipment in most nuclear medicine. NaI(Tl) properties has energy resolution of 7.2 , density of 3.67 g/cm^3 and decay time of 230 ns [51].

2.6.4 Explosives detection field

In this field the materials detection system made up with a NaI (Tl) gamma detectors and D-D neutron generators. These approach is used to analyze the response of the system to different materials (different samples) of explosive, for example NH_4NO_3 . The generator D-D can produce fast neutrons that greatly contribute to the detection of the explosives in the field national security. This method (procedure) allows to determine the type of substance and its chemical composition [26].

Chapter Three

Practical part

3.1 Introduction

This work deals with description of the electronic counting and analysis system using the scintillation detector and the study every part of it and its preparation for the purpose of obtaining the best and accurate practical results. This research includes an explanation of the spectrum regions, standard radioactive sources, and the geometric arrangement.

3.2 Electronic counting and analysis system: The electronic counting and analysis system used to detect nuclear radiation and equipped by Spectrum Techniques Company type (UCS-30) and using NaI(Tl) crystal by size (2×2) Inch figures (3.1) and (3.2) shown block diagram and realistic picture for counting system.

3.2.1 Preamplifier: In the an electronic device that receive the charge coming from the detector and converted it to a current pulse the current pulse to the voltage pulse and amplifier the voltage pulse [52].

3.2.2 Main amplifier: The main amplifier amplification the pulse out from the preamplifier to a level that can be analyzed from the multichannel analyzer (MCA) [53].

3.2.3 High Voltage power supply: The high voltage equipment works with the required voltage in these study its 700 volt.

3.2.4 Multi-Channel Analyzer (MCA): The Multi-Channel Analyzer (MCA) used in this study is an advanced devices in the study of gamma ray spectra, supplied by (Spectrum Techniques LLC). It contains 4096 channels It is characterized by its high ability analyze gamma spectra. The (MCA) converts the pulse coming from the main amplifier into the digital numbers. The system, reduce the exposure time to ray and simplify the real time check of the spectrum [54].

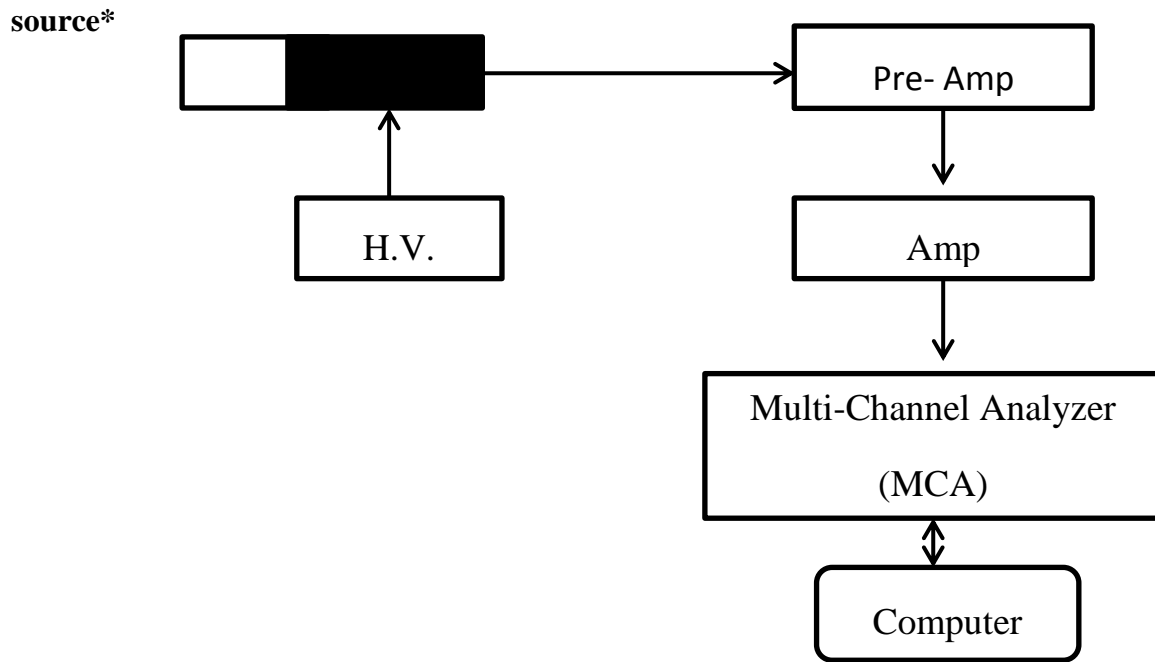


Figure (3.1) The Block diagram of the counting system.

Also a realistic picture of the system as shown in figure (3.2).

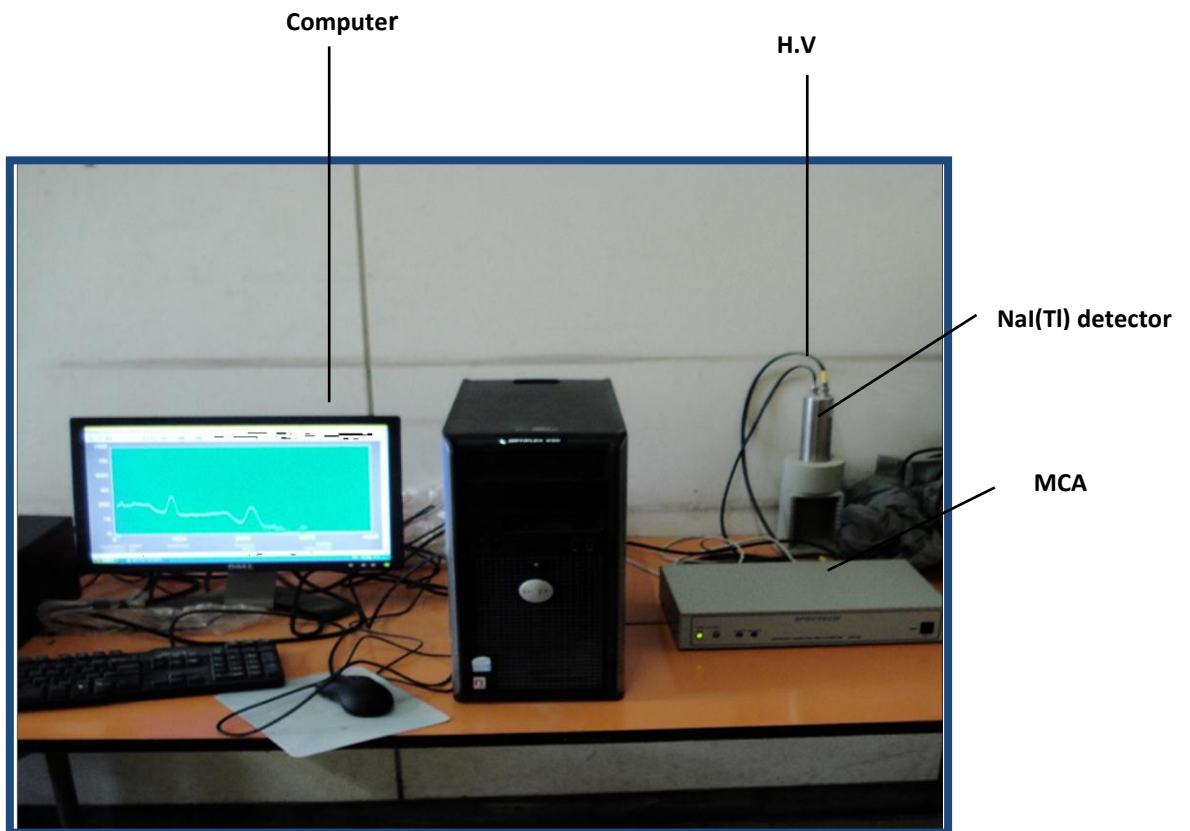


Figure (3.2) Counting and analysis system.

3.3 Radioactive Source: Used Cs-137 with an energy of (0.662 MeV), Na 22 with energies (0.511MeV and 1.276MeV) and Co- 60 with energies (1.173 MeV and 1.332MeV) as shown in the Table (3.1).

Table (3.1) the radioactive sources used in experimental part.

Radioactivity Sources	Activity (μci)	Half-life (year)	Energy (MeV)
Cs- 137	0.889	30.7	0.662
Na- 22	0.191	2.6	0.511
Na- 22	0.191	2.6	1.276
Co-60	0.442	5.27	1.173
Co-60	0.442	5.27	1.333

The scintillation detector is used to detect gamma rays on the assumption that the gamma spectrum is linear because it is single-energy, and this spectrum contains peaks or a continuous distribution depending on the nature of the interaction, and each reaction show one or more of peak, and this is due to the energy of the interacting photon [52]. Figures(3.3) ,(3.4) and (3.5) represent the spectra of elements that were used in the practical aspect with collection time 1000 sec.

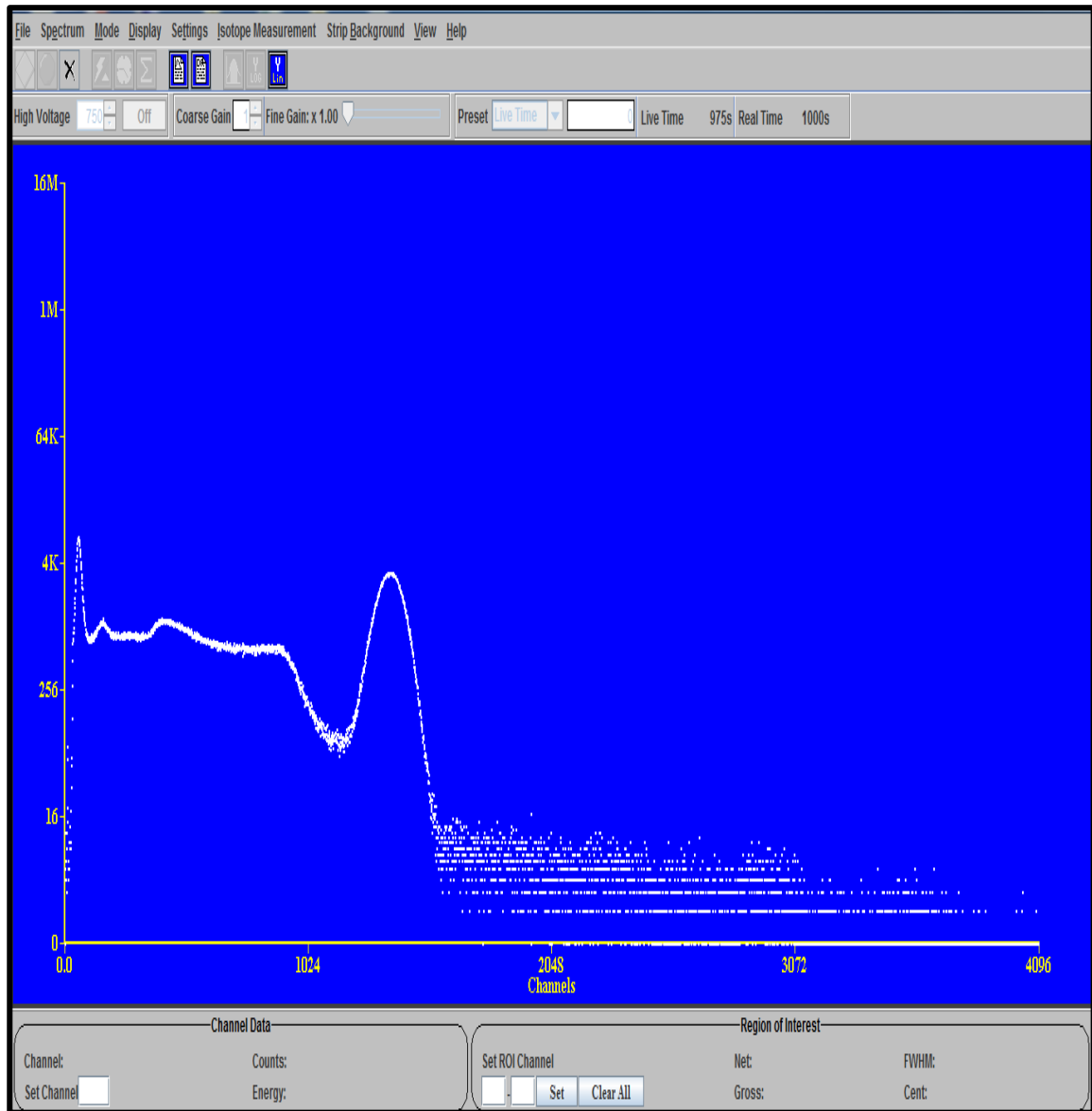


Figure (3.3) Cs – 137 spectrum.

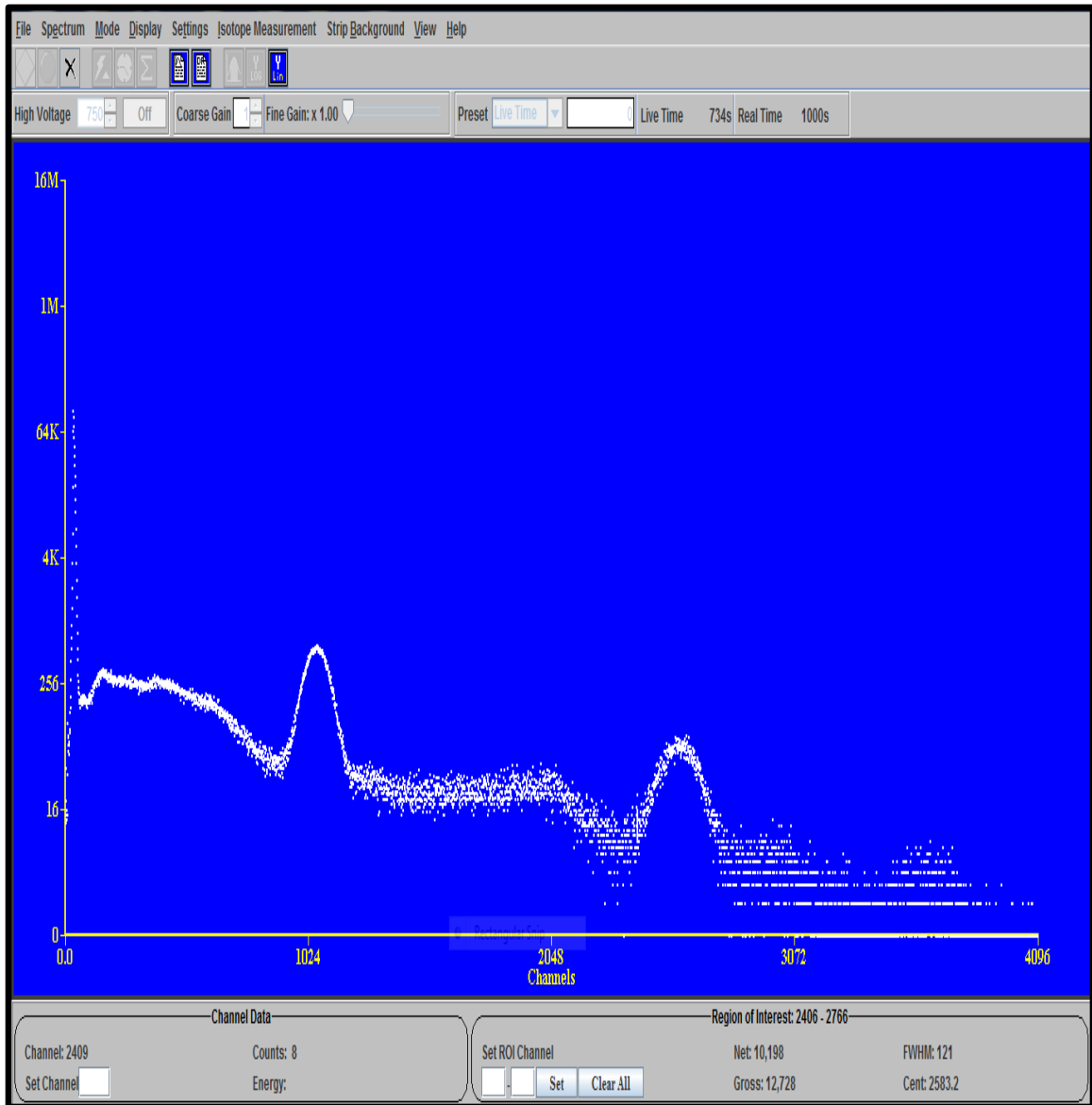


Figure (3.4) Na- 22 spectrum.

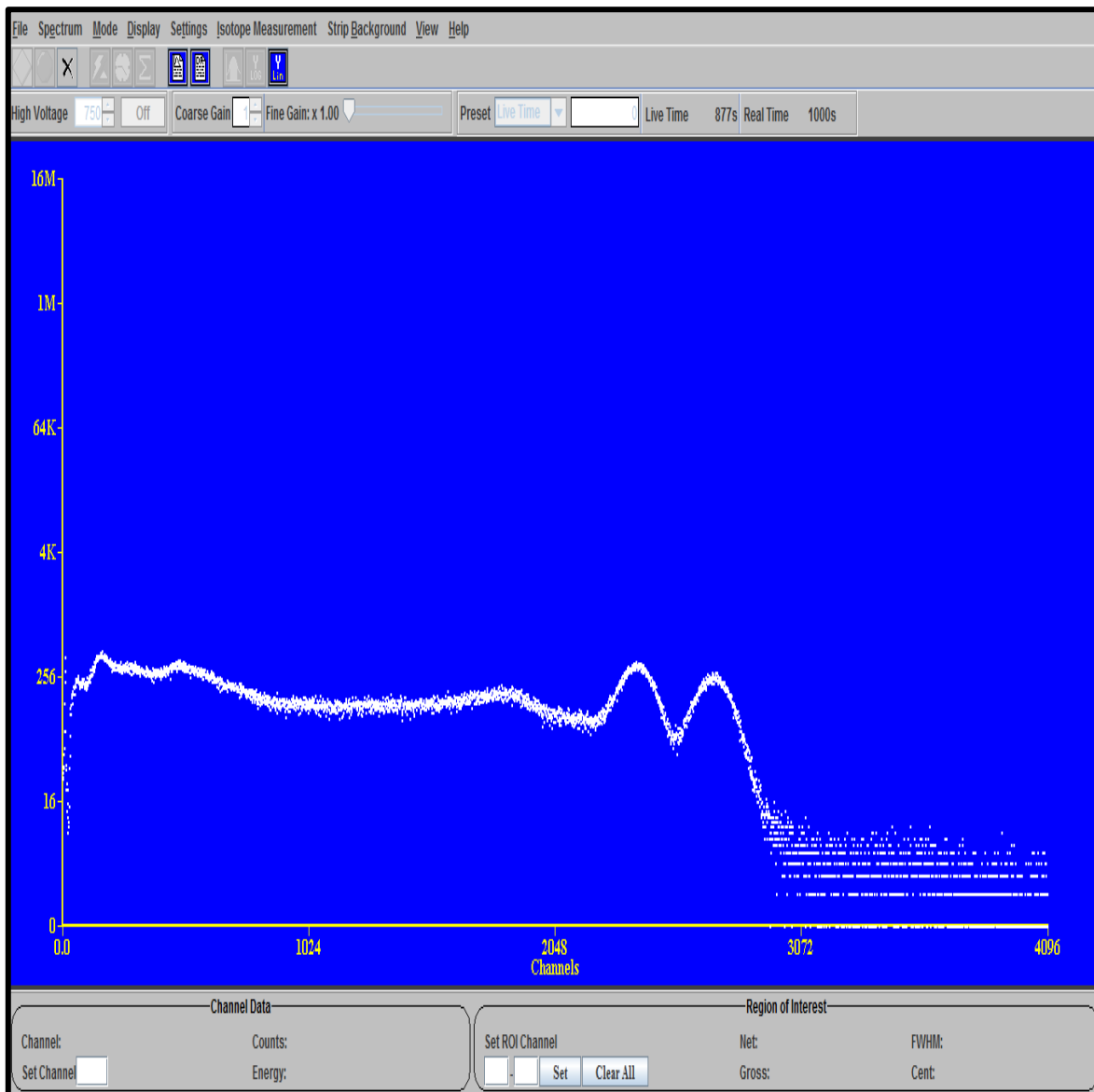


Figure (3.5) Co – 60 spectrum.

3.4 Geometric configuration

An electric heat source was used that raised the temperature by five degree Celsius starting from 15°C and 20°C degrees until a temperature 45°C . The distance between the detector and heat source is 45cm, and used two thermometers to measure the temperatures, each one of them was 15cm away from the detector from each beside. A container coated with a temperature preservative used the container to containing the detector, the radioactive source the heat source and thermometers for purpose to stay the temperature longest possible period and to obtain the best result as shown in figure (3.6).

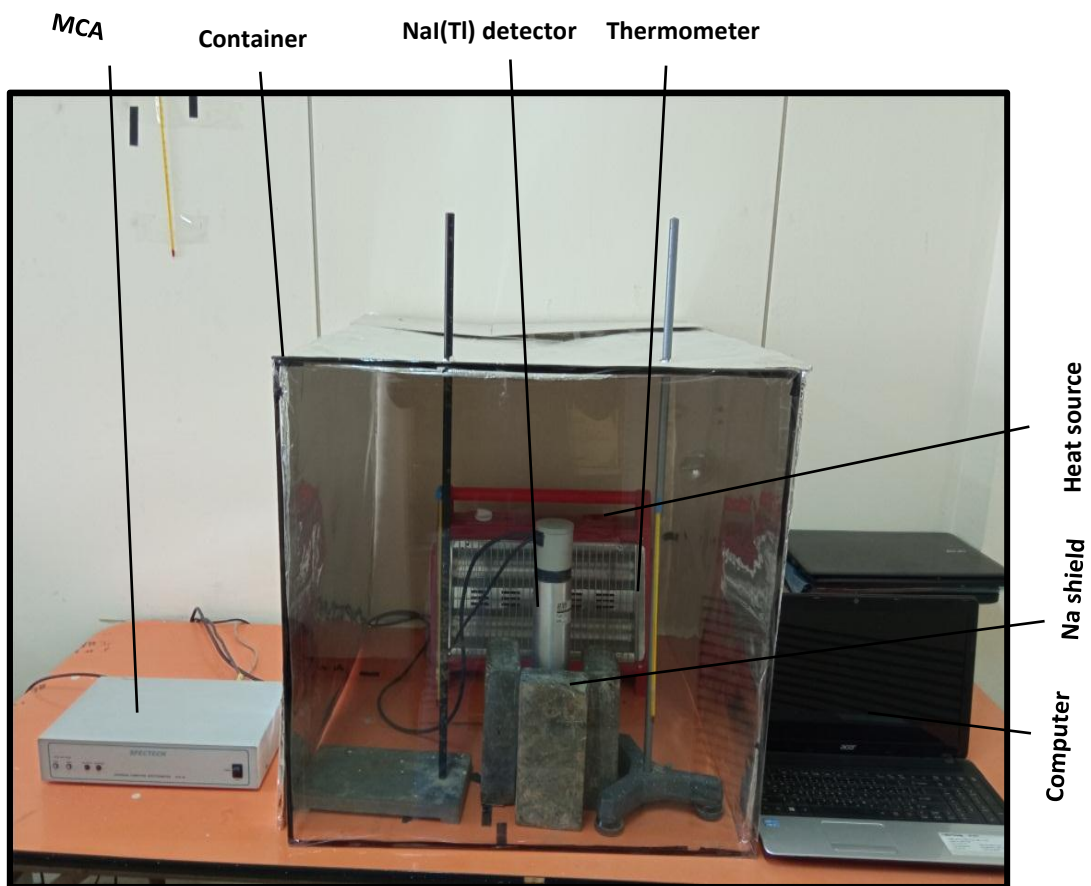


Figure (3.6) Geometric configuration.

Chapter Four
Results, Discussions,
Conclusions and
Suggestions

The results obtained from the practical side mentioned and discussion in this chapter. All results for all radioactive resource measured with time (1000 sec)

4.1 Cs-137

Cesium (Cs-137) is one of the sources that have been used in the practical experiments in this research , and its experimental results are shown in Table (4.1).

Energy resolution (E.R)

It the ability of detector to analysis the particles or photons it have different energies .The energy resolution represented by (E.R) and can be calculated by this equation(1) [41].

$$E.R = \frac{FWHM}{Cent.} \times 100\% \quad (4.1)$$

Where **FWHM** the full width half maximum.

Cent: the center point of the photo peak middle.

Photo peak: Represented full absorbs to energy of photon gamma ray inside detector crystal. The photo peak appearing in photoelectric interaction .

Total Area of spectrum : It number of the pulses for all channels and it measure by (count/sec).

Photo Peak Net Area: Its represent the start point of photo peak to the end point photo peak and the unit measure is (count/sec).

Table (4.1) The results of the present work for Cs-137.

Temperature	Total area		Photo peak (0.662 MeV)				
	Net c/sec	Gross c/sec	Net c/sec	Gross c/sec	FWHM ch.no.	Centroid ch.no.	E. R
20	1232±35	1243±35	410±20	423±21	118	1365	0.08644
25	1225±35	1241±35	408±20	422±21	116	1356	0.08554
30	1221±35	1237±35	407±20	421±21	114	1344	0.08482
35	1222±35	1236±35	406±20	421±21	116	1325	0.08754
40	1219±35	1237±35	405±20	422±21	114	1301	0.08762
45	1221± 35	1231±35	405±20	419±20	113	1268	0.08911

Table (4.1) show the results obtained from effect temperature change on total spectrum area and area photo peak1 with standard deviation for the radioactive element (Cs-137).

4.1.1 Total spectrum area

The effect of temperature on the total area of the Cs-137 spectrum .The effect of temperature on the net total area of the cesium spectrum and according to the results mentioned in Table (4.1), the relation between the change in the temperature and net total area is shown in figure(4.1).

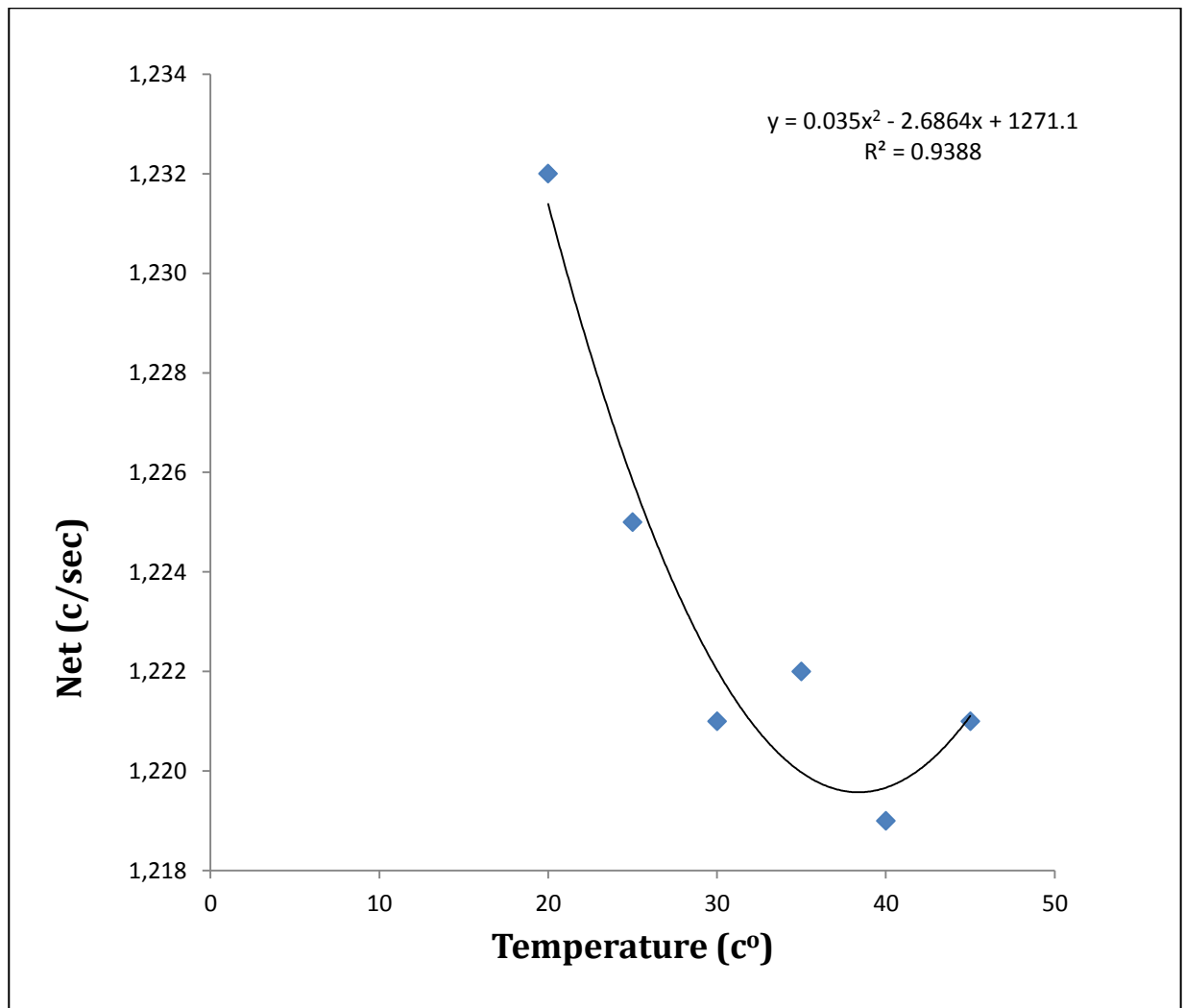


Figure (4.1) Distribution net count with change temperature for Cs-137 total area.

From figure (4.1) found the general behavior inverse proportionality, when temperature increases the net count decreases due decrease in the number of photon for to the net spectrum total area across the detector and that is disagreement with previous study [40].

The effect of temperature on the total area of the Cs-137 spectrum .The effect of temperature on the gross total area of the cesium spectrum and according to the results mentioned in Table (4.1), the relation between the change in temperature and gross total area is shown in figure (4.2).

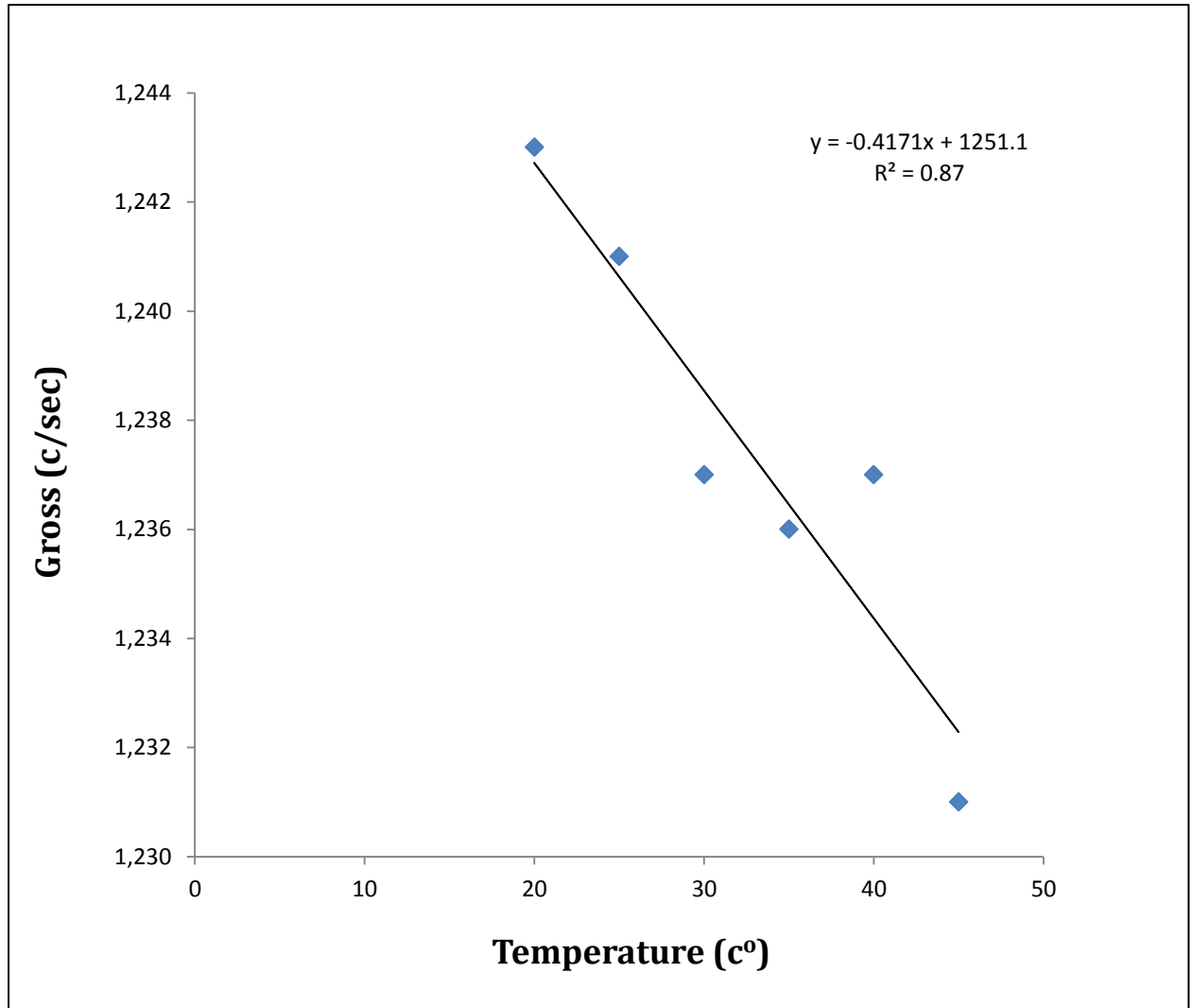


Figure (4.2) Distribution gross count with change temperature for Cs-137 total area.

From figure (4.2) notice in general that count decrease with increasing temperature due decrease in the number of photons for to the gross spectrum total area across the detector due of the change in temperature, and these result better from previous study [40].

4.1.2 Photo peak at (0.662 MeV)

The effect of temperature on the net photo peak area of the Cs-137 spectrum the effect of temperature on the net photo peak of the cesium spectrum and according to the results mentioned in Table (4.1), the relation between the change in the temperature and net photo peak is drawn as shown in figure (4.3).

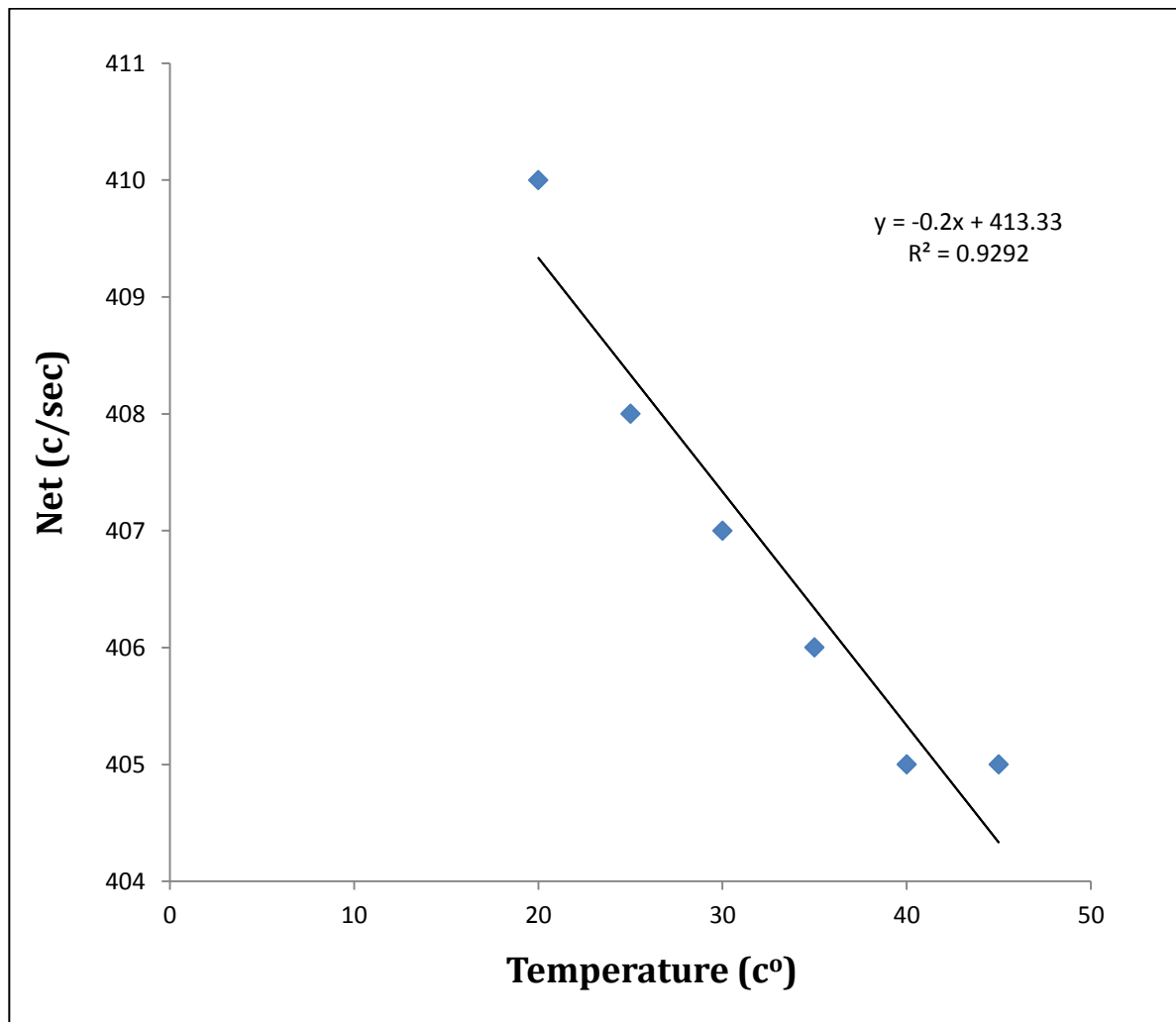


Figure (4.3) Distribution the net count with change temperature for Cs-137 photo peak.

From figure (4.3) linear relation between net and temperature(inverse proportionality) that is due loss information because decrease in the amount of light resulting from interaction radiation with detector crystal and that is disagreement and better from previous study [40].

The effect of temperature on the gross photo peak area for the Cs-137 spectrum. The effect of temperature on the gross photo peak of the cesium spectrum and according to the results mentioned in Table (4.1), the relation between the change in the temperature and gross photo peak as shown in figure (4.4).

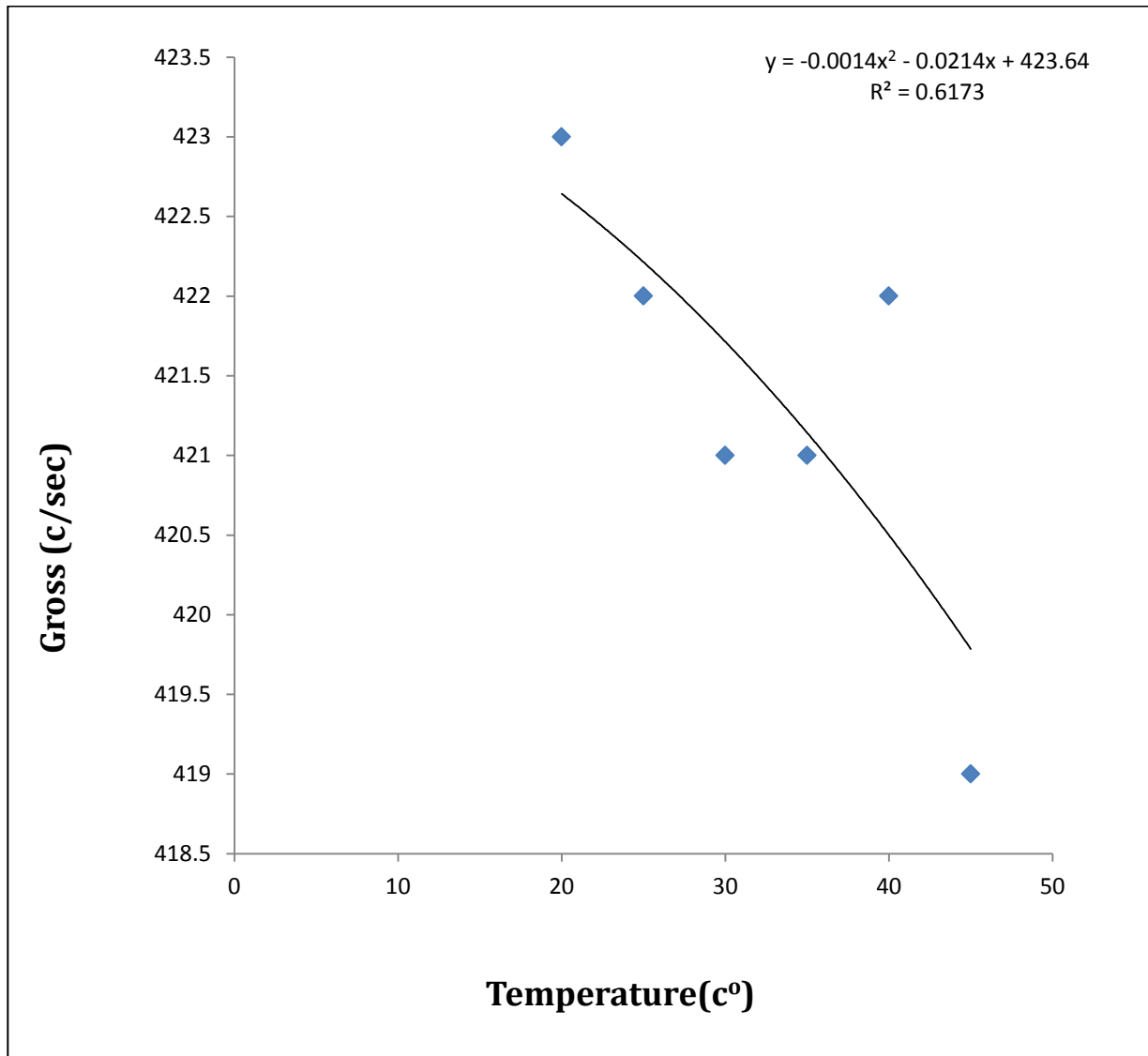


Figure (4.4) Distribution the gross count with change temperature for Cs-137 photo peak.

From figure (4.4) the general behavior is the count decrease when temperature increases (inverse relation between temperature and Gross photo peak) due loss photons by effect temperature change and that is disagreement and better from previous study [40].

The effect of temperature on the FWHM photo peak area for the Cs-137 spectrum. The effect of temperature on the FWHM photo peak of the cesium spectrum and according to the results mentioned in Table (4.1), the relation between the change in the temperature and FWHM photo peak as shown in figure (4.5).

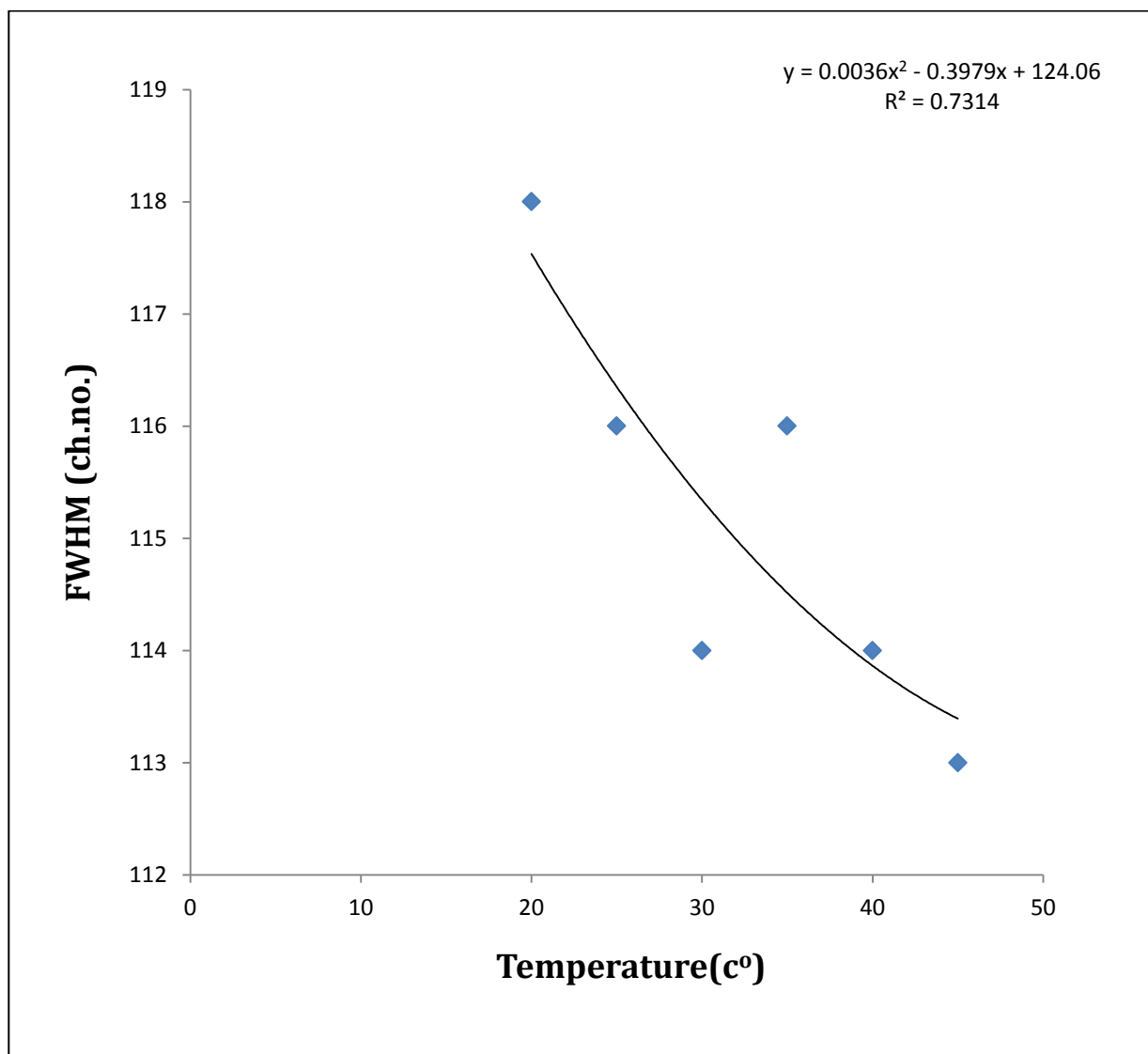


Figure (4.5) Distribution the FWHM with change temperature for (Cs-137) photo peak.

From figure (4.5), the relation between the FWHM photo peak and temperature has inverse relation that is due to the increase in temperature and the spectrum is compressed into lower channels, causing decrease in the width of the mid-photo peak.

The effect of temperature on the position photo peak area for the Cs-137 spectrum. The effect of temperature on the position photo peak of the cesium spectrum and according to the results mentioned in Table (4.1), the relation between the change in the temperature and position photo peak as shown in figure(4.6).

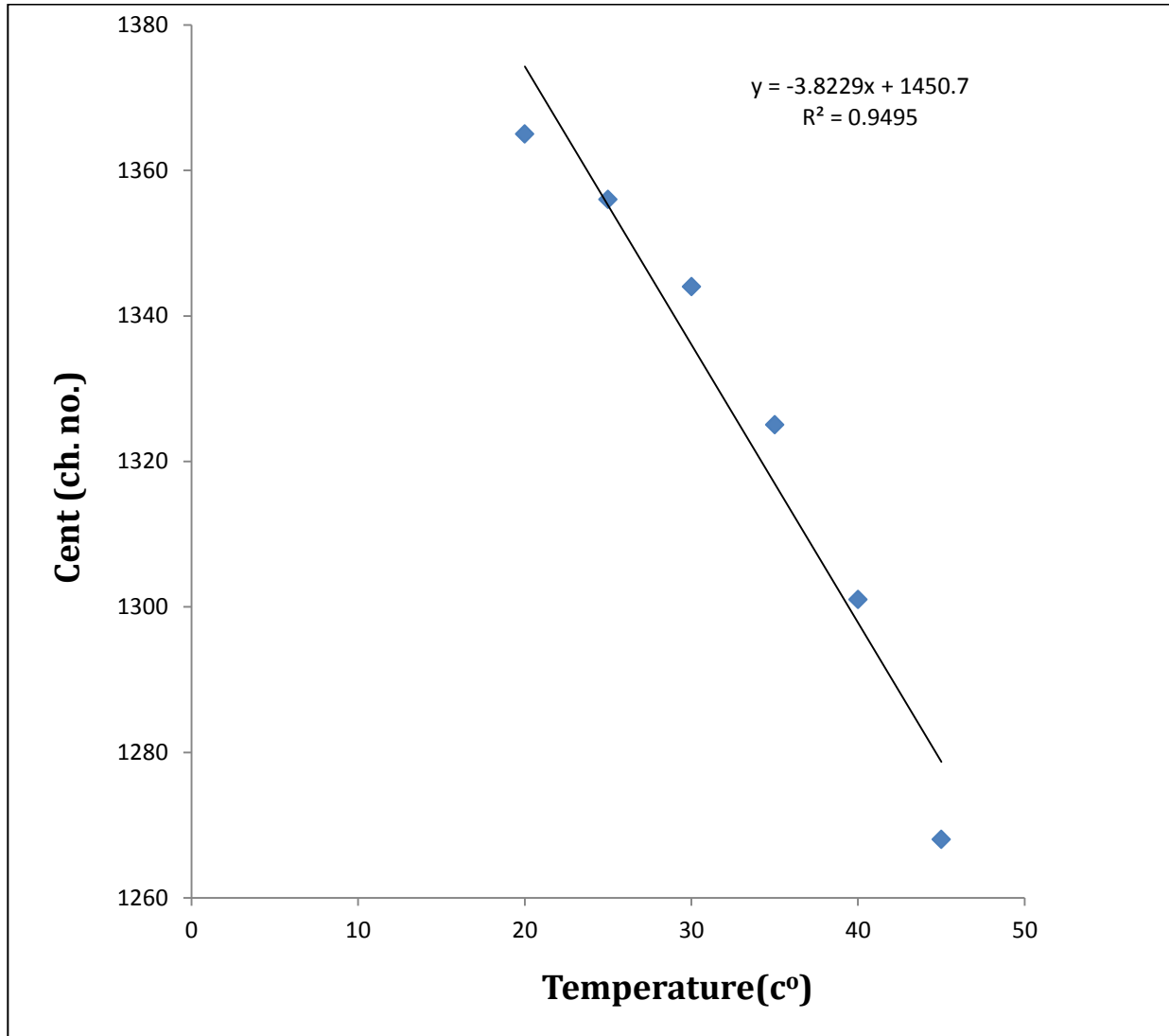


Figure (4.6) Distribution the position photo peak (centroid) with change temperature for (Cs-137) photo peak.

From figure (4.6) the relation between temperature and position photo peak, it inverse proportionality, when temperature increases the centroid move to the lower channels levels due spectrum compression due to the change in temperature. This agreed with previous study[40].

The effect (T) on the E.R for the Cs-137 spectrum according to the results mentioned in Table (4.1), the relation between the change in the temperature and E.R as shown in figure (4.7) .

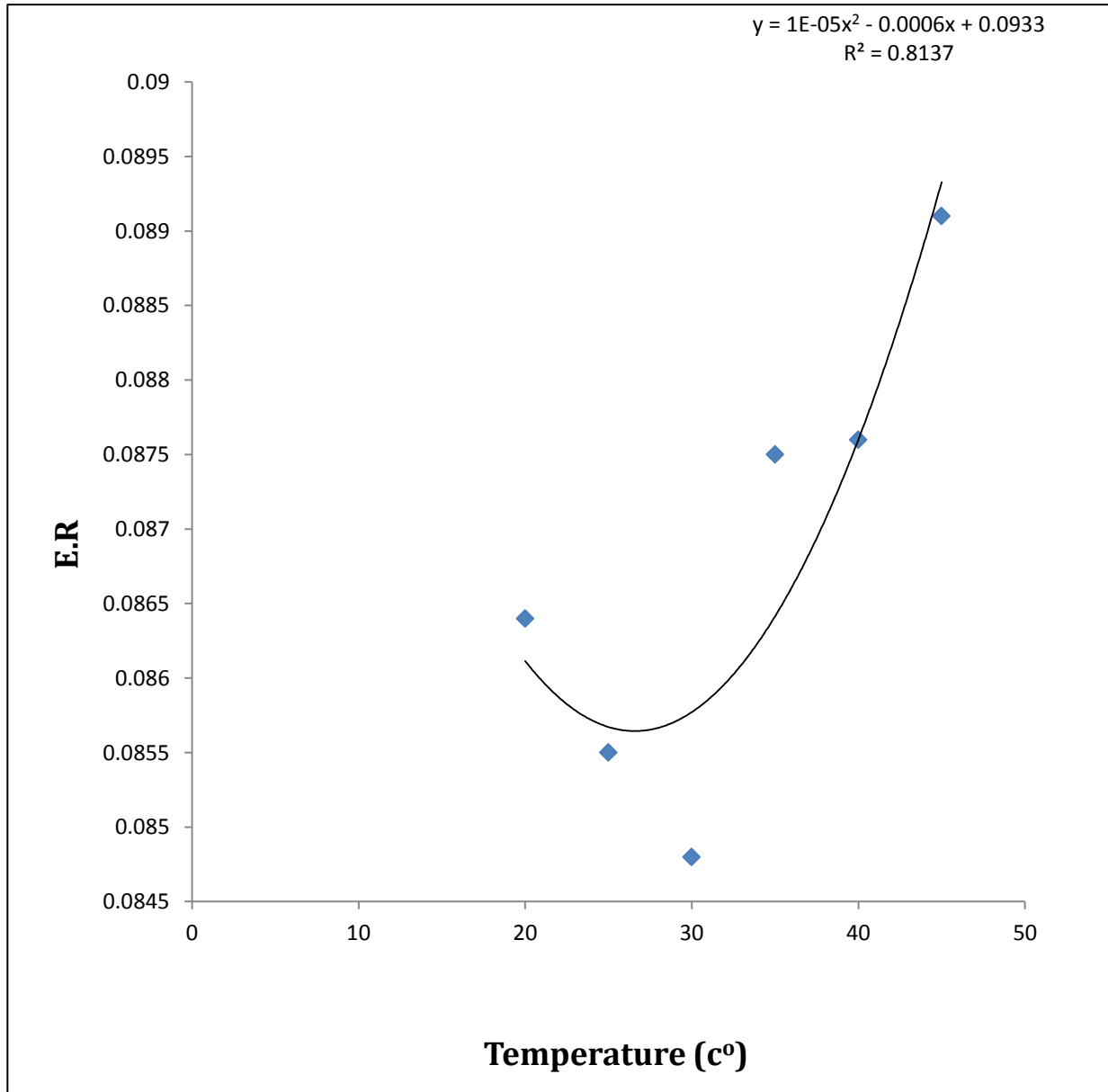


Figure (4.7) Distribution the E.R with change temperature for (Cs-137) photo peak.

From figure (4.7) the relation between the E.R photo peak and temperature has no clear behavior (incomprehensible behavior) due the E.R dependence on the ratio between FWHM and centroid and these ratio gives disproportionate results.

4.2. Na-22

Sodium (Na-22) was also used in practical experiments in this research, and its results are shown in Table (4.2).

Table (4.2) the results effect of temperature on the total area and first photo peak for Na-22.

Temperature	Total Area		Photo Peak1 (0.511 MeV)				
	Net c/sec	Gross c/sec	Net c/sec	Gross c/sec	FWHM ch.no.	centroid ch.no.	E.R
15	174±13	193±14	65±8	73±9	95	1068	0.0889
20	685±26	832±29	59±8	68±8	102	1057	0.0964
25	1524±39	1549±39	52±7	60±8	103	1055	0.0976
30	2730±52	2879±54	45±7	52±7	108	1048	0.1030
35	2823±52	2878±54	44±7	52±7	102	1033	0.0987
40	2812±53	2880±54	43±7	51±7	106	1015	0.1044
45	2922±54	2897±54	43±7	50±7	90	983	0.09155

Table (4.2) show the results obtained from effect temperature change on the total spectrum area and area photo peak1 with standard deviation for the radioactive element (Na-22) .

4.2.1 Total Area

The effect of temperature on the net area for the Na-22 spectrum .The effect of temperature on the net of the Na-22 spectrum and according to the results mentioned in Table (4.2) , the relation between the change in the temperature and net as shown in figure (4.8).

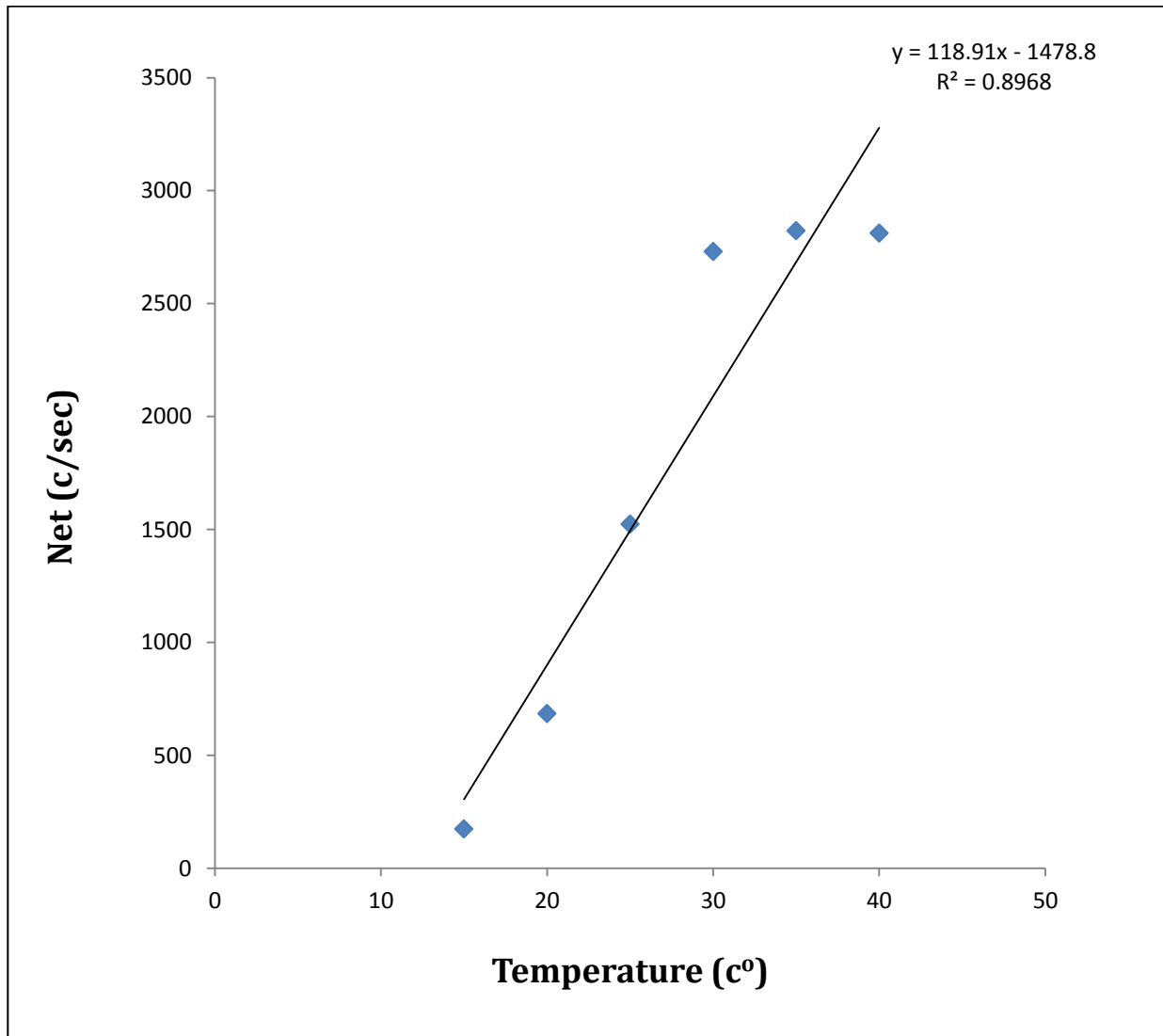


Figure (4.8) Distribution the net with change temperature for (Na-22) for total area.

From figure (4.8), the general behavior between net count and temperature is different behavior than before due reversed work and cooling was used instead of heating.

The effect of temperature on the gross area for the Na-22 spectrum .The effect of temperature on the gross of the Na-22 spectrum and according to the results mentioned in Table (4.2), the relation between the change in the temperature and gross as shown in figure (4.9).

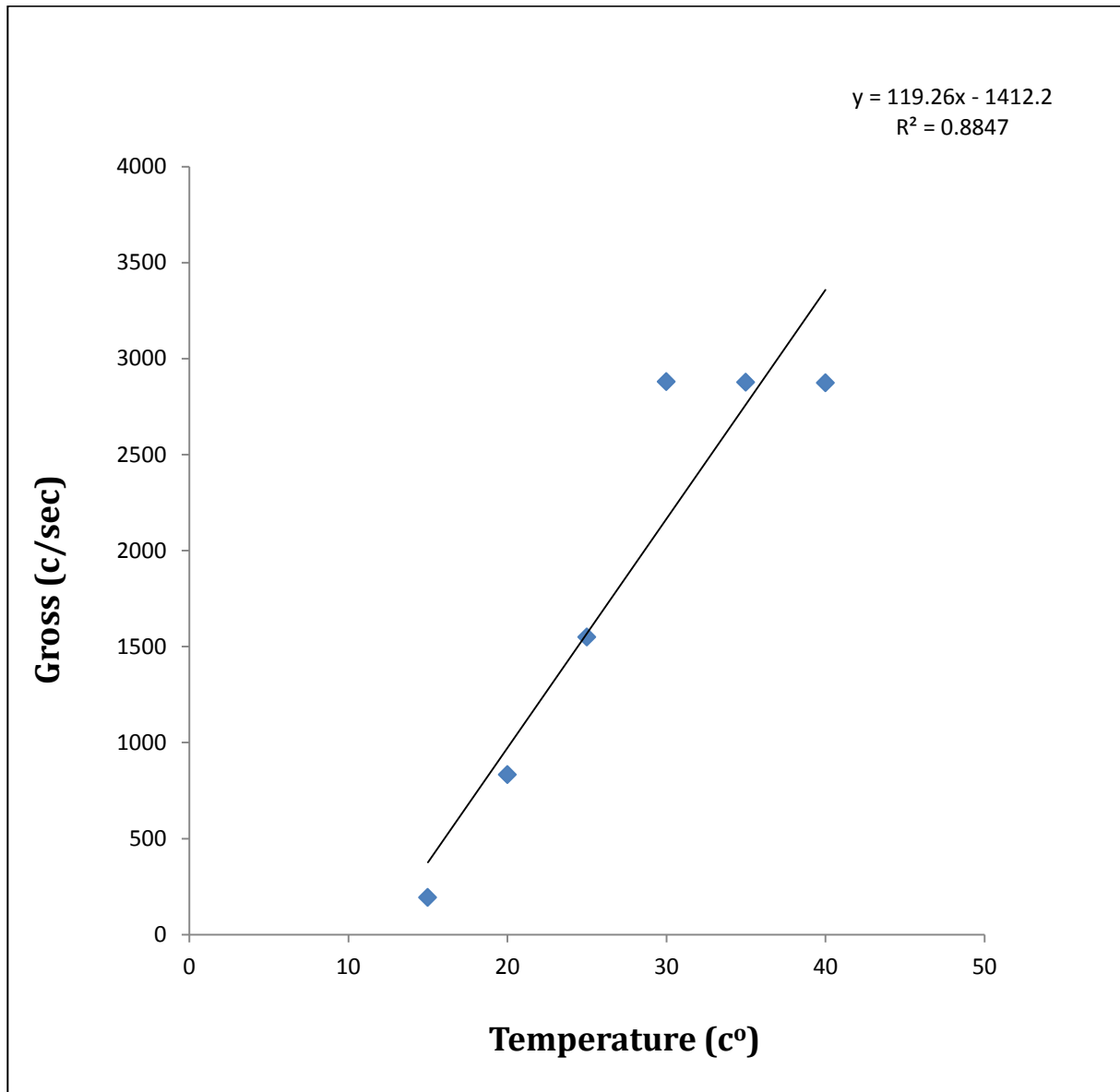


Figure (4.9) Distribution the gross with change temperature for (Na-22) for total area.

From figure(4.9), the general behavior between gross count and temperature is direct proportionality due reversed work and cooling was used instead of heating this reduces the effect of temperature.

4.2.2 Photo peak 1 at (0.511 MeV)

The effect of temperature on the net area for the Na-22 spectrum. The effect of temperature on the net of the Na-22 spectrum and according to the results mentioned in Table (4.2), the relation between the change in the temperature and net as shown in figure (4.10).

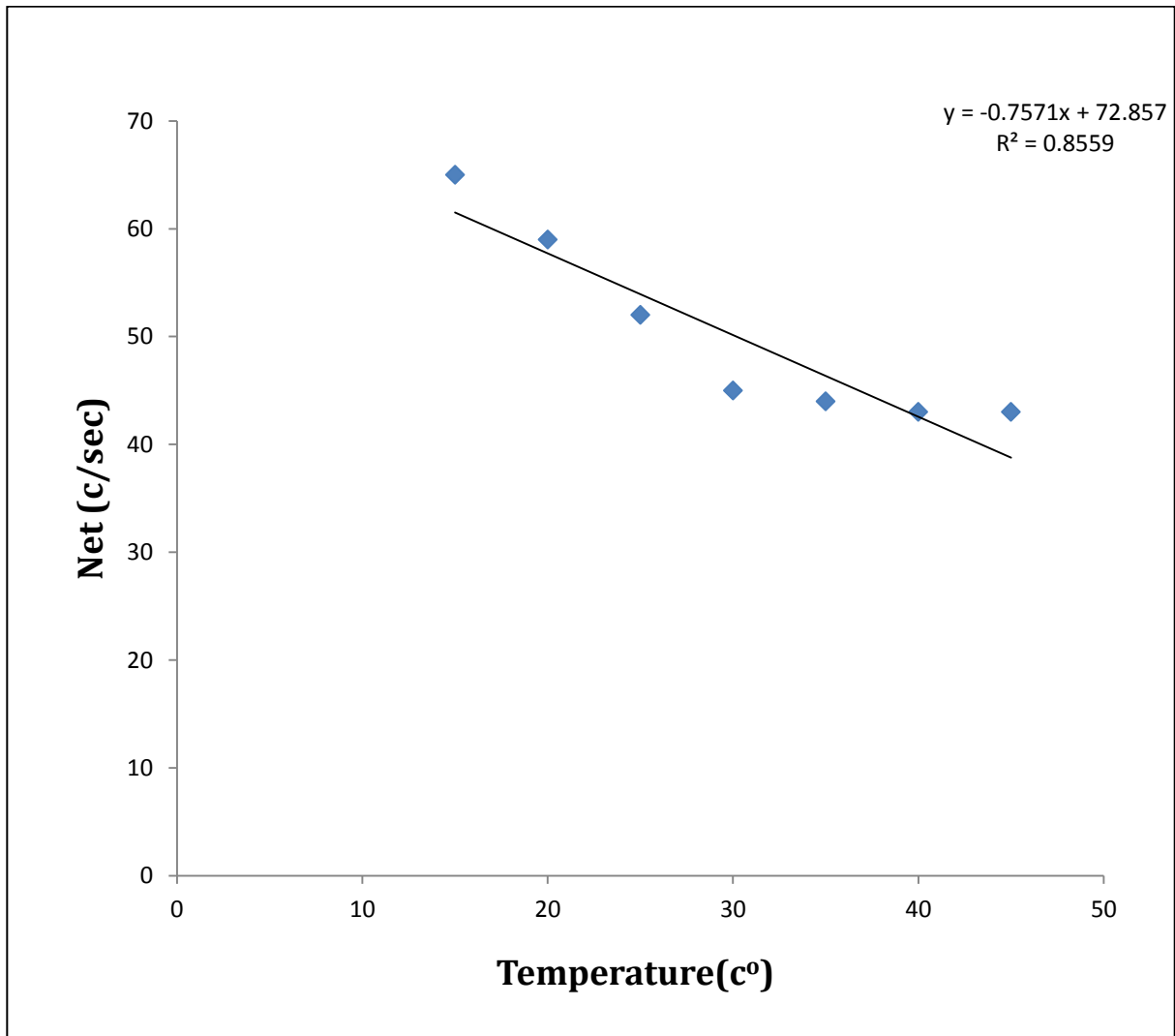


Figure (4.10) Distribution the net with change temperature for(Na-22) photo peak1.

From figure (4.10) , when temperature increases the net count for photo peak1 decreases due to the scintillation pulse generated decrease for net photo peak area when temperature increase and that is disagreement with previous study [40].

The effect of temperature on the gross area for the Na-22 spectrum. The effect of temperature on the gross of the Na-22 spectrum and according to the results mentioned in Table (4.2), the relation between the change in the temperature and gross as shown in figure (4.11).

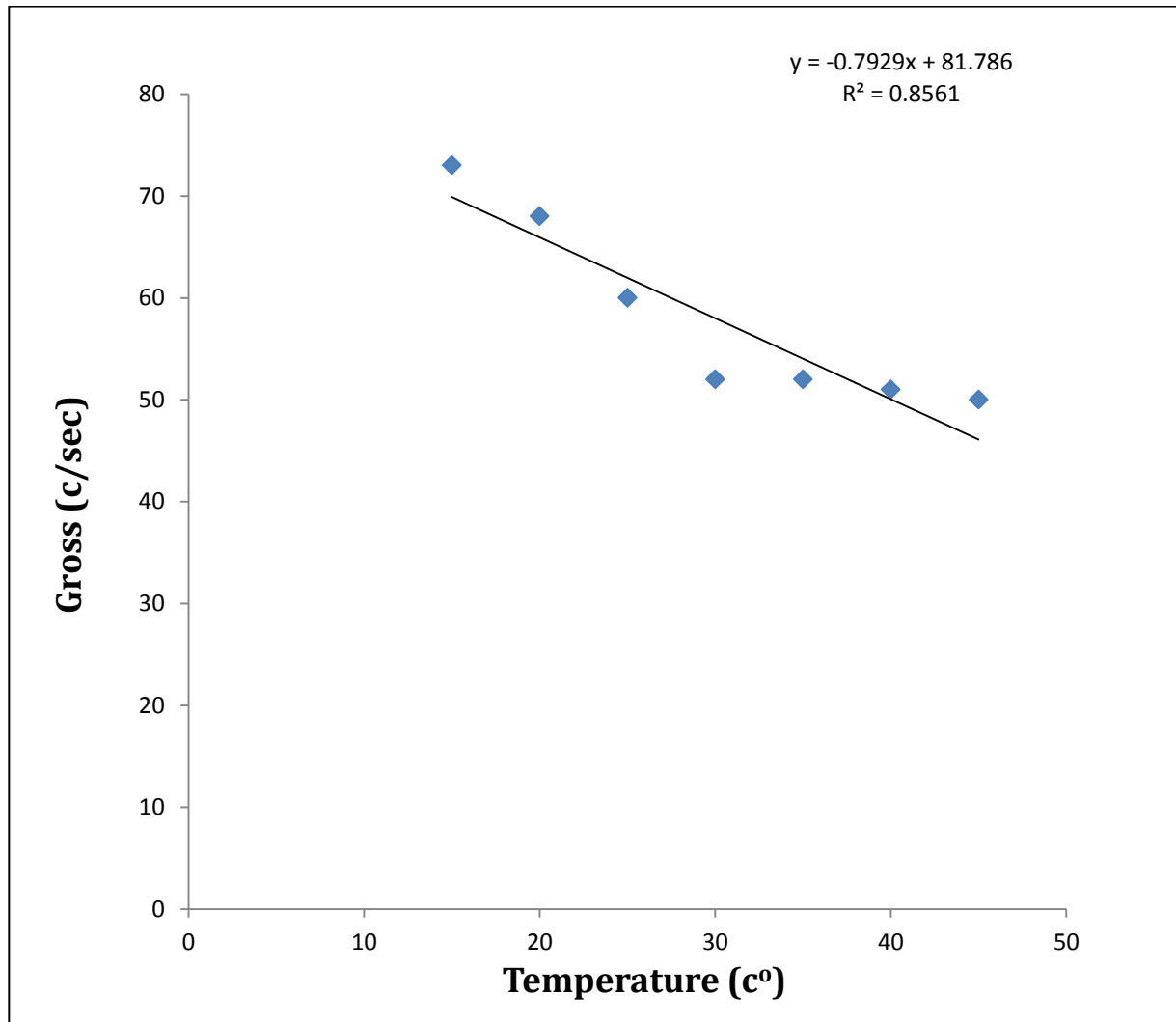


Figure (4.11) Distribution the gross with change temperature for (Na-22) photo peak1.

From figure (4.11), when temperature increases the gross count for photo peak1 due to the scintillation pulse generated decrease for gross photo peak area when temperature increase and that is disagreement with previous study [40].

The effect of temperature on the FWHM area for the Na-22 spectrum .The effect of temperature on the FWHM of the Na-22 spectrum and according to the results mentioned in Table (4.2), the relation between the change in the temperature and FWHM as shown in figure (4.12).

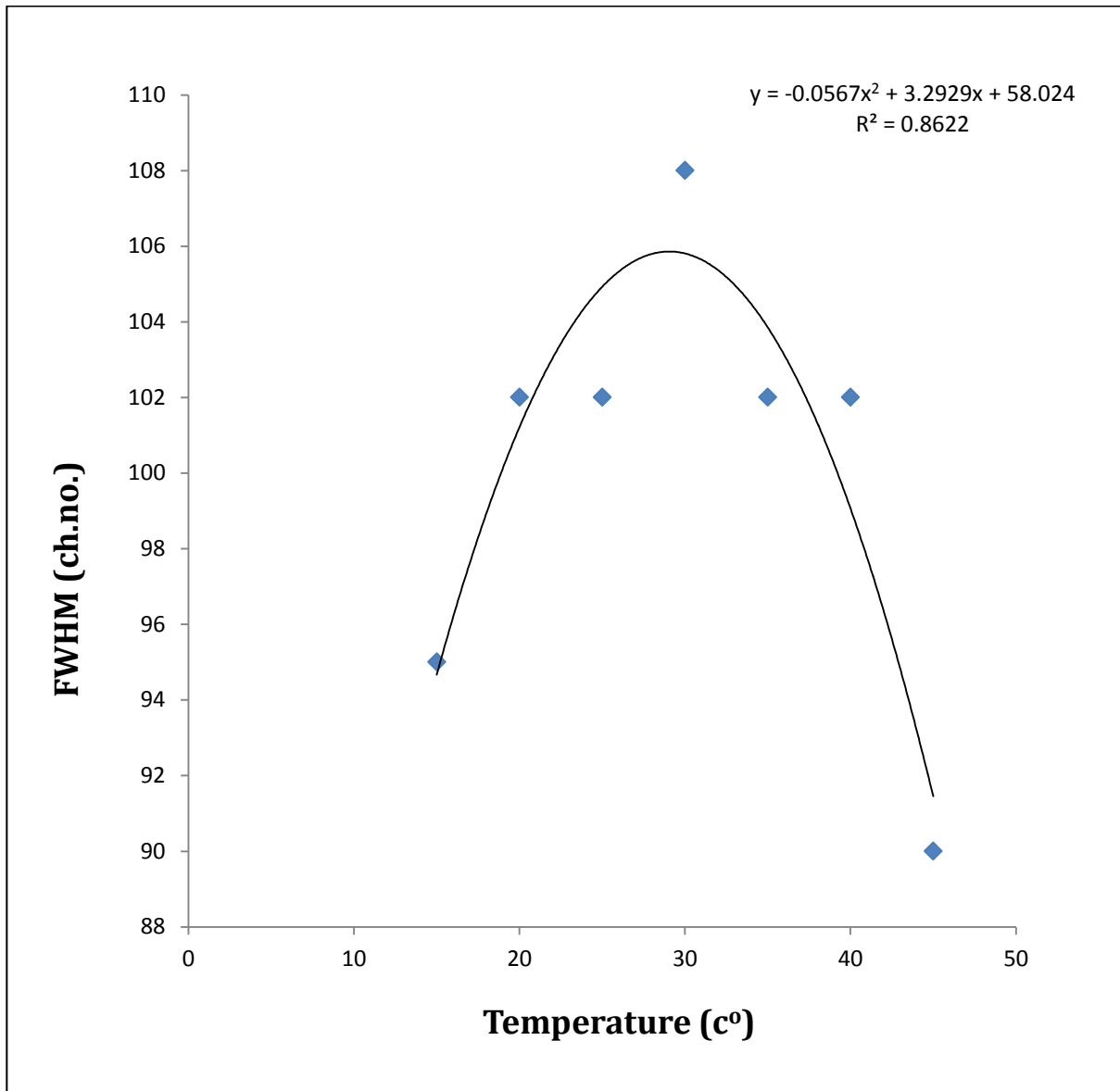


Figure (4.12) Distribution the FWHM with change temperature for(Na-22) photo peak1.

From figure (4.12), the relation between the FWHM and temperature has no clear behavior due Na-22 has positrons involved and its annihilation emits a photon by 0.511 MeV.

The effect of temperature on the position photo peak for the Na-22 spectrum according to the results mentioned in Table (4.2), the relation between the change in the temperature and position photo peak as shown in figure (4.13).

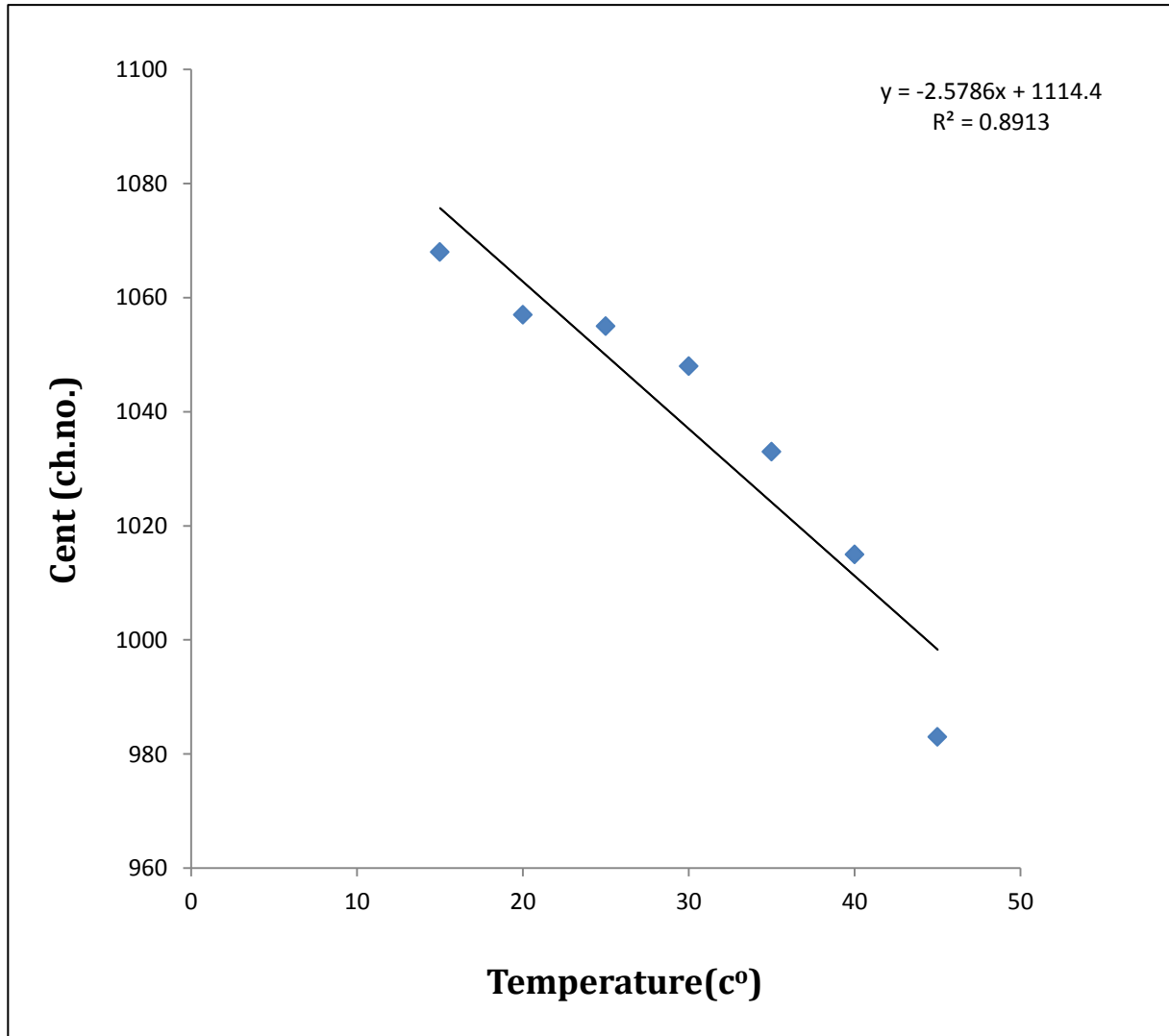


Figure (4.13) Distribution the centroid with change temperature for(Na-22) photo peak1.

From figure (4.13), the relation between the temperature and position photo peak inverse proportionality, due the spectrum compression when the temperature increase that is cause the centroid photo peak1 to move into lower channels levels. This agreed with previous study[40].

The effect of temperature on the (E.R) for Na-22 spectrum according to the results mentioned in Table (4.2), the relation between the change in the temperature and (E.R) as shown in figure (4.14).

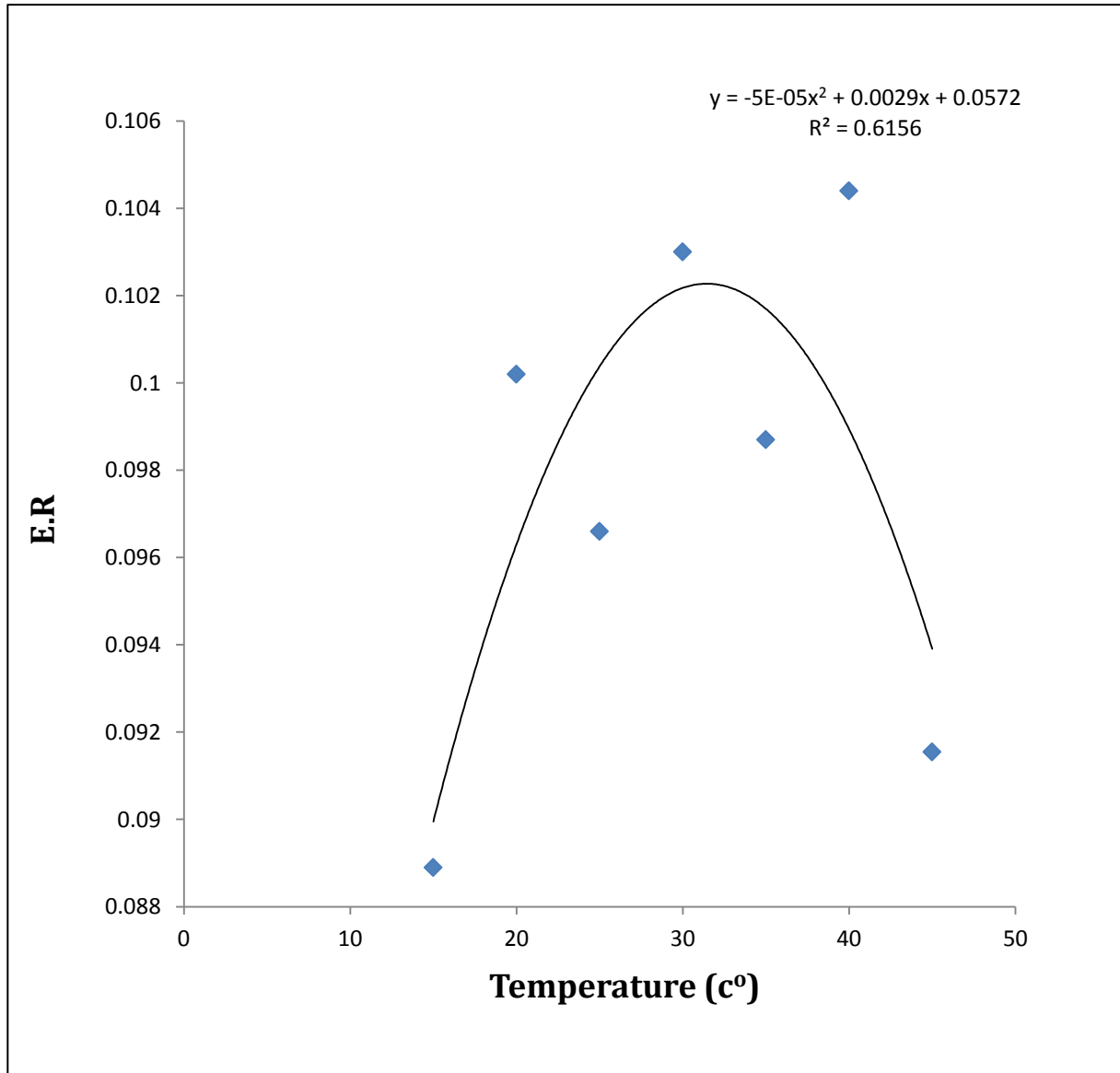


Figure (4.14) Distribution the E.R with change temperature for(Na-22) photo peak1.

From figure (4.14) , the relation between the E.R and increases temperature has no clear behavior due the energy resolution dependence on the ratio for photo peak1 between FWHM and position photo peak (centroid) .

4.2.3 Photo peak 2 at (1.276 MeV)

The effect of temperature on the second photo peak of Na-22 was studied, and these results are shown in Table (4.3)

Table (4.3) the results of the effect of temperature on the second photo peak of Na-22.

Temperature	Photo peak2 (1.276 MeV)				
	T (C ⁰)	Net (c/sec)	Gross (c/sec)	FWHM (ch.no.)	centroid (ch.no.)
15	11±4	13±4	119	2610	0.0455
20	10±3	12±3	121	2584	0.0468
25	9±3	10±3	108	2576	0.0419
30	8±3	9±3	58	2555	0.0227
35	8±3	9±3	44	2518	0.0174
40	7±3	8±3	41	2474	0.0165
45	6±3	7±3	110	2405	0.0457

Table (4.3) show the results obtained from effect temperature change on the area photo peak1 for the radioactive element (Na-22) in addition to the standard deviation.

The influence of temperature on the net photo peak₂ for the Na-22 spectrum that is according to the results mentioned in Table (4.3), the relation between the change in the temperature and net as shown in figure (4.15).

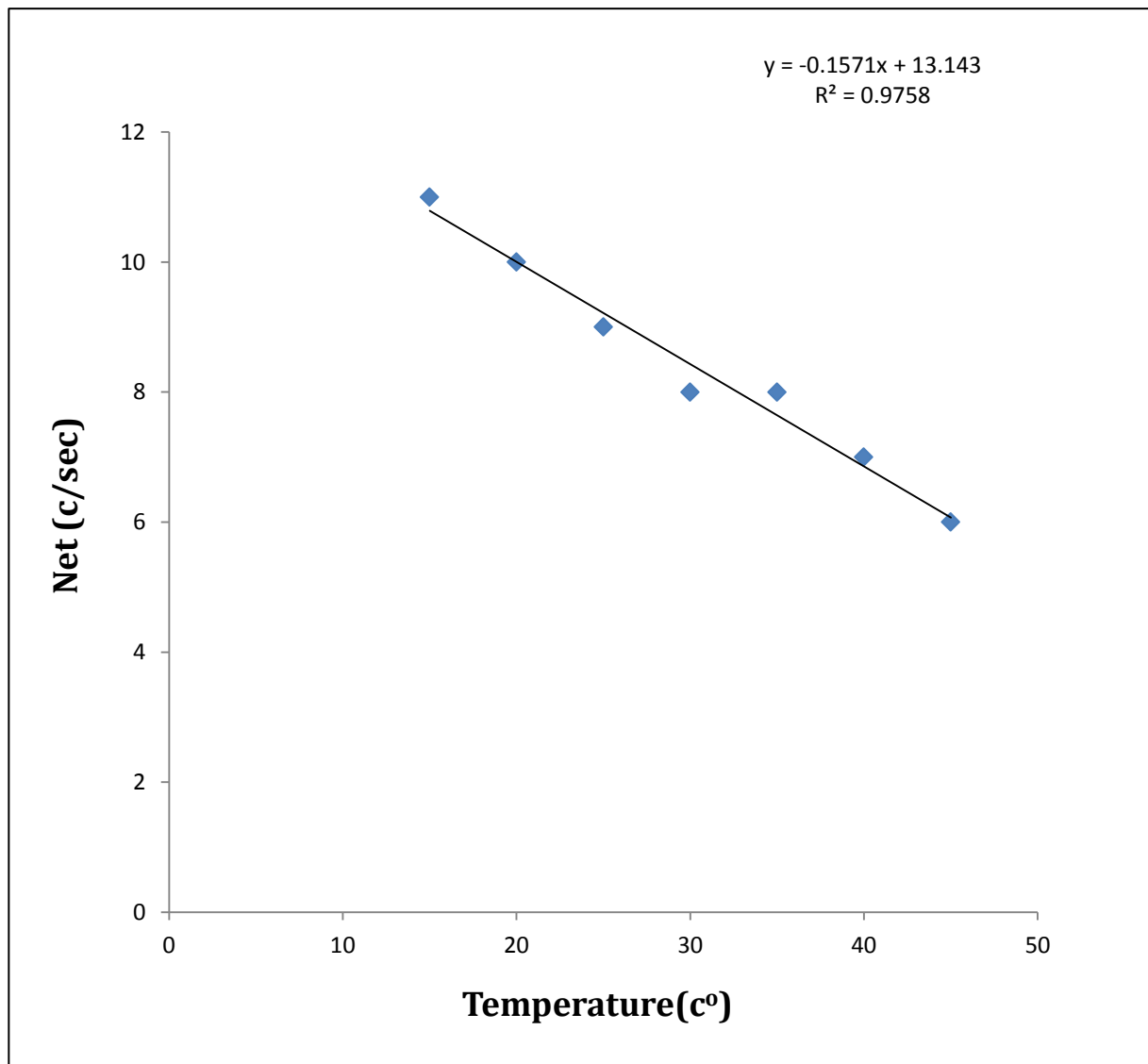


Figure (4.15) Distribution the net with change temperature for (Na-22) photo peak₂.

From figure (4.15) when temperature increases the net count decreases. (inverse proportionality) because decrease in the scintillation pulse generated due increase in the temperature and that is disagreement but better from previous study [40].

The influence of (T) on the gross photo peak2 for the Na-22 spectrum, the effect of temperature on the gross of the Na-22 spectrum and according to the results mentioned in Table (4.3), the relation between the change in the temperature and gross as shown in figure (4.16).

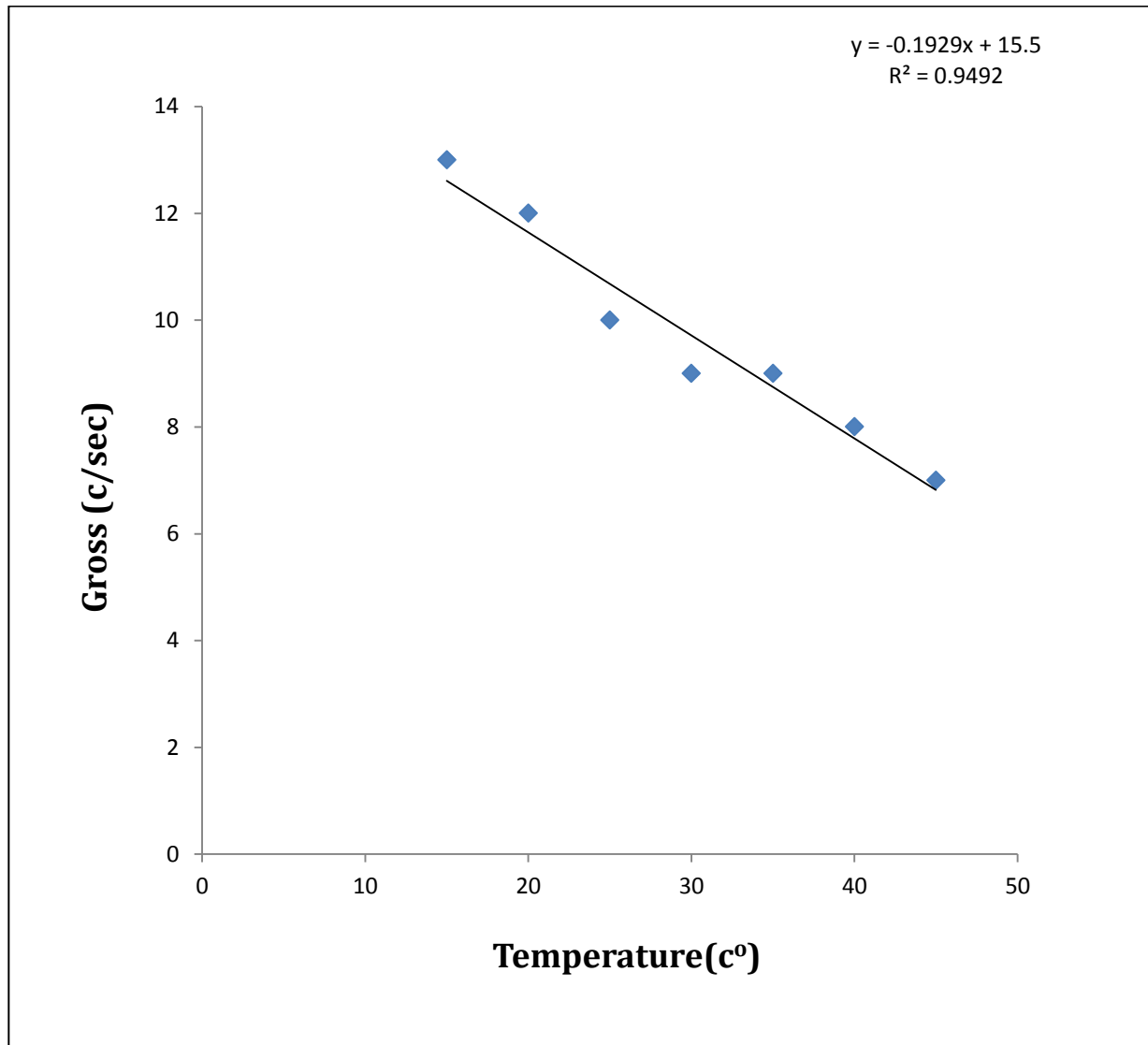


Figure (4.16) Distribution the gross with change temperature for (Na-22) photo peak2.

From figure (4.16), when temperature increases the gross count decreases. (inverse proportionality) that is back to the loss interaction photons when temperature increase and that is disagreement with previous study [40].

The effect of temperature on the FWHM photo peak2 for the Na-22 spectrum, effect of temperature on the FWHM of the Na-22 spectrum and according to the results mentioned in Table (4.3), the relationship between the change in the temperature and FWHM as shown in figure (4.17).

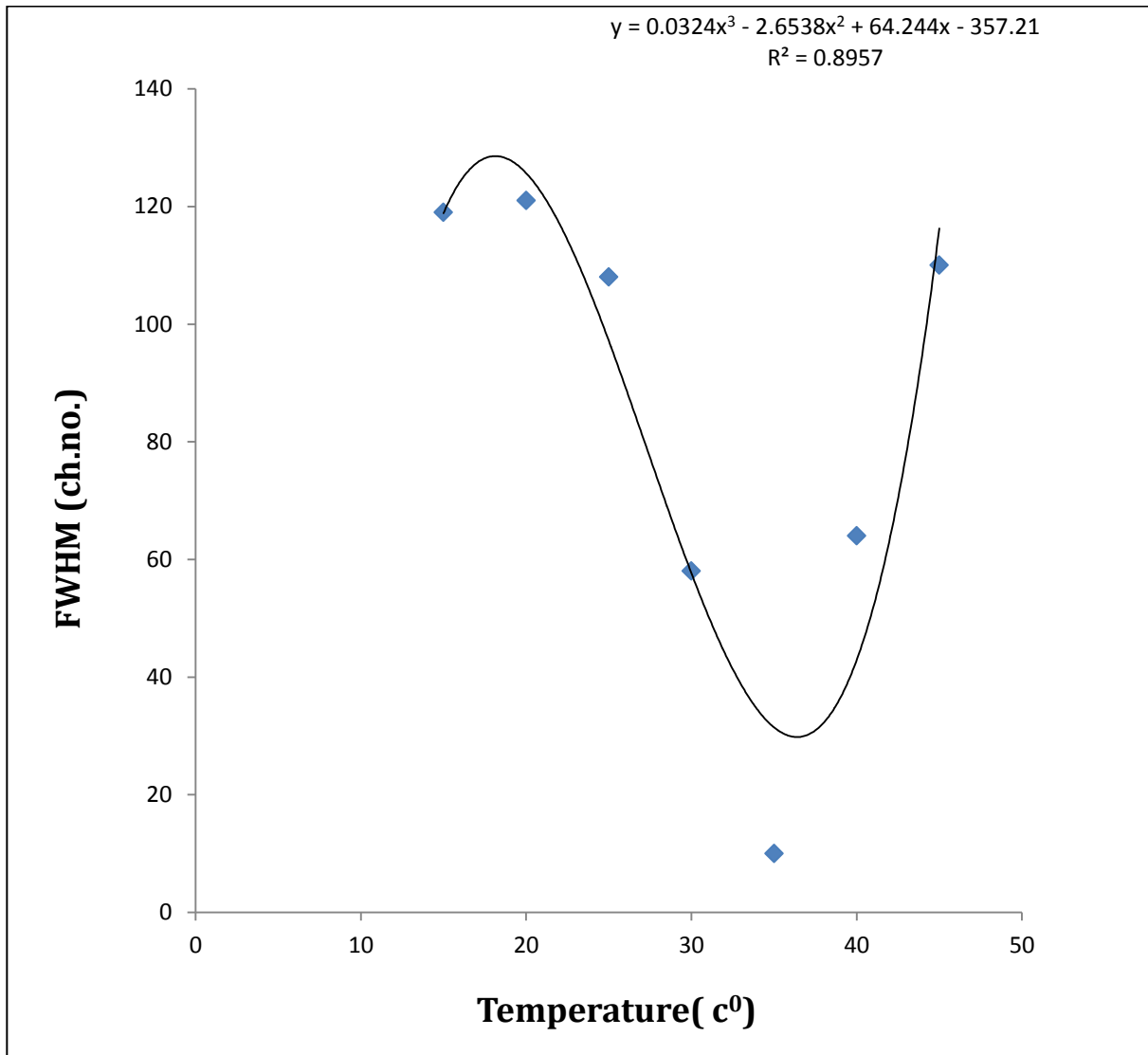


Figure (4.17) Distribution FWHM with change temperature for(Na-22) photo peak2.

From figure (4.17), found that the relation between the FWHM and temperature has no clear behavior (incomprehensible behavior) due the Na-22 emit positron addition to the photon therefore the increase in temperature effect on this emission.

The effect of temperature on the position photo peak2 for the Na-22 spectrum, the effect of temperature on the position of the Na-22 spectrum and according to the results mentioned in Table (4.3), the relation between the change in the temperature and FWHM is drawn as shown in figure (4.18).

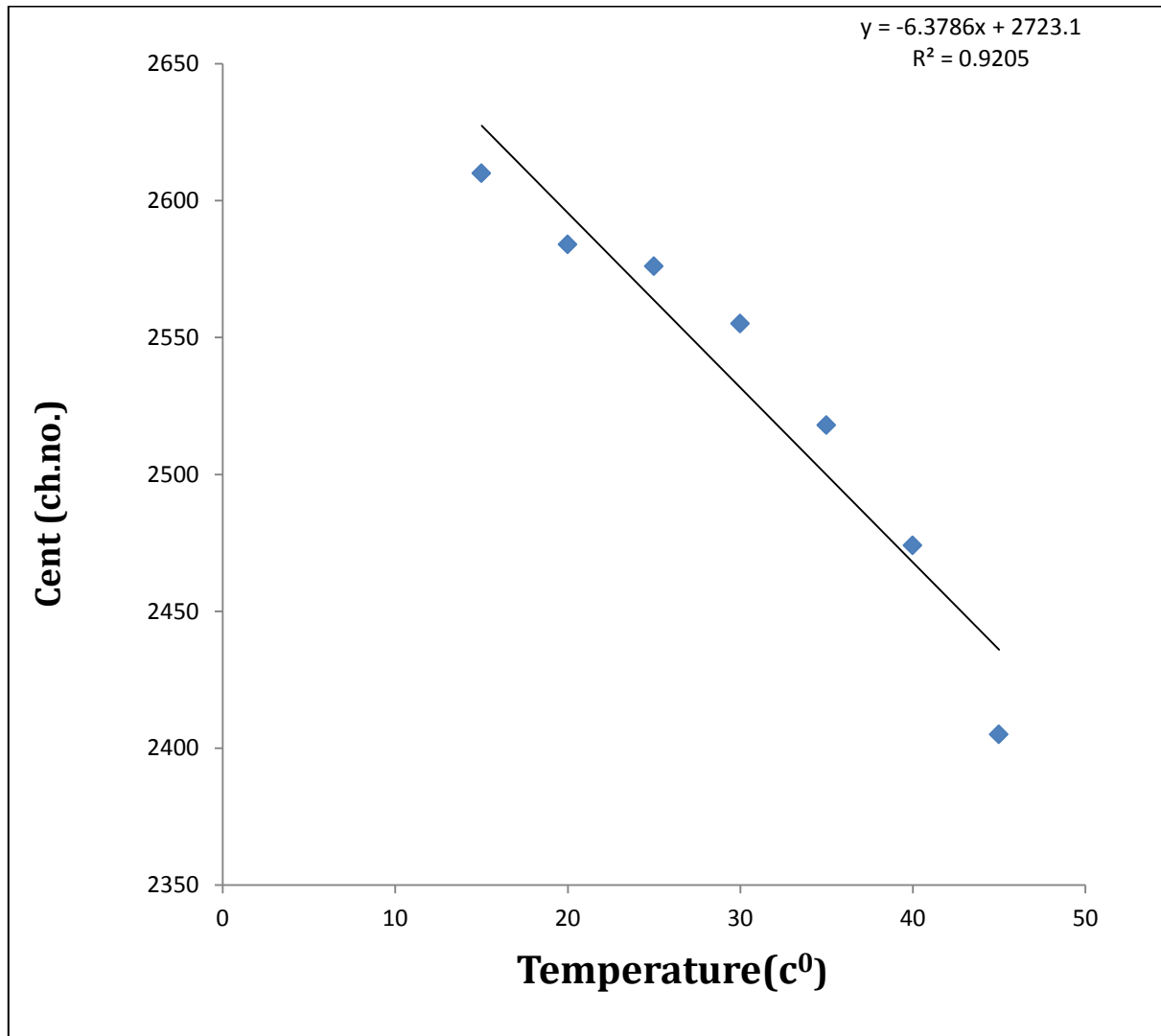


Figure (4.18) Distribution the centroid with change temperature for(Na-22) photo peak2.

From figure (4.18), the relation between the temperature and position photo peak, when temperature increases the centroid move to the lower channel levels due the output spectrum pulse compression . This agreed with previous study[40].

The effect (T) on the energy resolution E.R photo peak2 for the sodium spectrum . Influence of temperature on the E.R of the Na-22 spectrum and according to the results mentioned in Table (4.3), the relation between change in temperature and E.R as shown in figure (4.19).

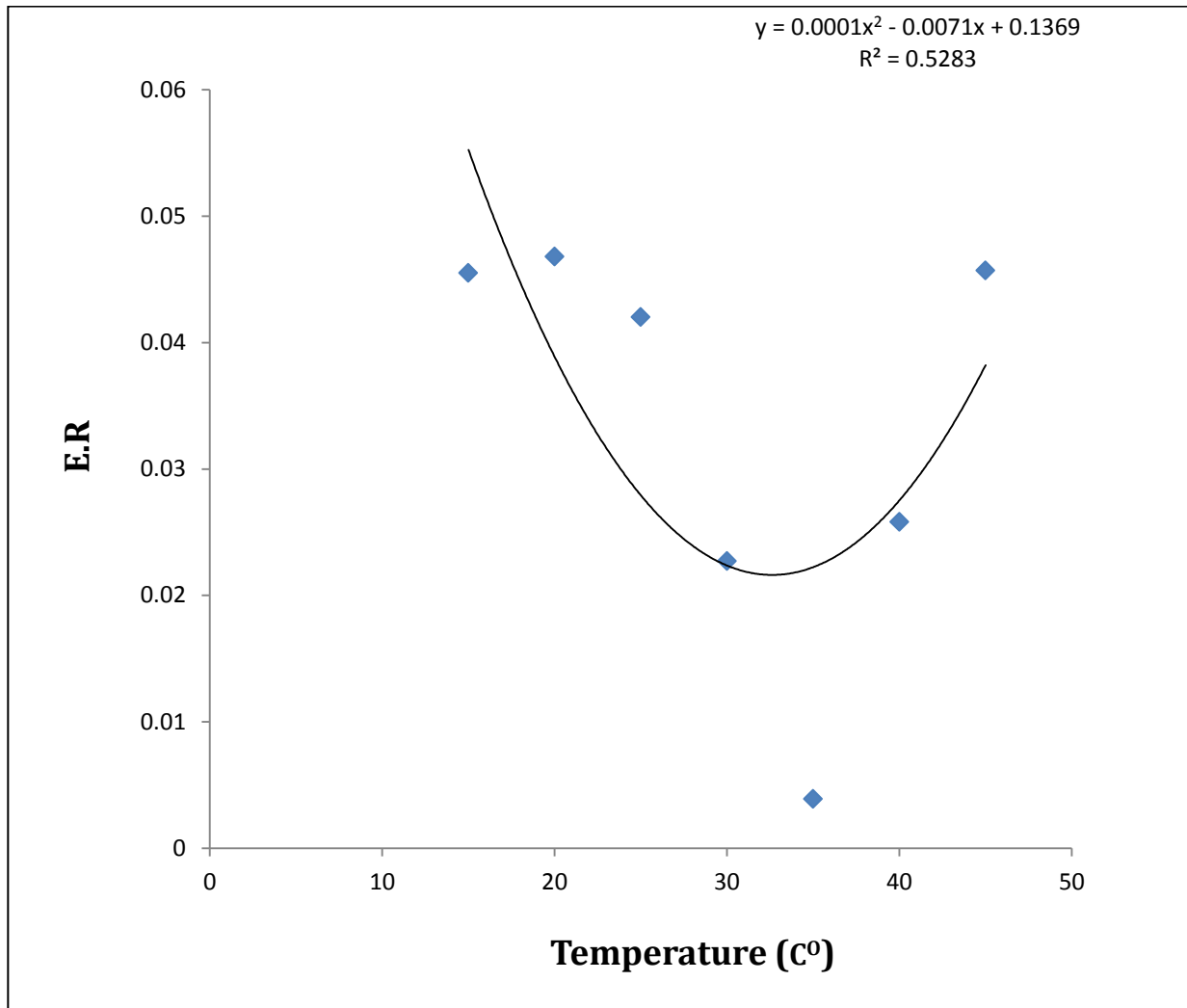


Figure (4.19) Distribution the E.R with change temperature for(Na-22) photo peak2.

From figure (4.19), there is no clear behavior from the effect of temperature on energy resolution (E. R) because the different in the ratio between FWHM and centroid for photopeak2 .

4.3 Co-60

The effect of temperature on the total spectrum area and first photo peak for Cobalt (Co-60) was studied, and these results are shown in Table (4.4) .

Table (4.4) the results of the effect of temperature on the total area and first photo peak for (Co-60).

Temperature	Total area		Photo peak1 (1.173 MeV)				
	Net c/sec	Gross c/sec	Net c/sec	Gross c/sec	FWHM ch.no.	centroid ch.no.	E.R
15	364±19	427±21	38±6	61±8	137	2406	0.0548
20	363±19	425±21	37±6	61±8	132	2379	0.0554
25	320±18	435±22	38±6	60±8	112	2358	0.0474
30	278±17	424±21	36±6	59±8	126	2312	0.0549
35	338±18	421±21	36±6	58±8	111	2291	0.0484
40	330±18	420±20	35±6	57±8	122	2251	0.0541
45	269±16	419±20	34±6	56±7	124	2182	0.0591

Table (4.4) show the results obtained from effect temperature change on the total spectrum area and area photo peak1 for the radioactive element (C0-60) in addition to the standard deviation.

4.3.1 Total Area

Study the effect of temperature on the net for total area to the Co-60. The effect of temperature on the net of the Co-60 spectrum and according to the results mentioned in Table (4.4), the relation between the change in the temperature and net as shown in figure (4.20).

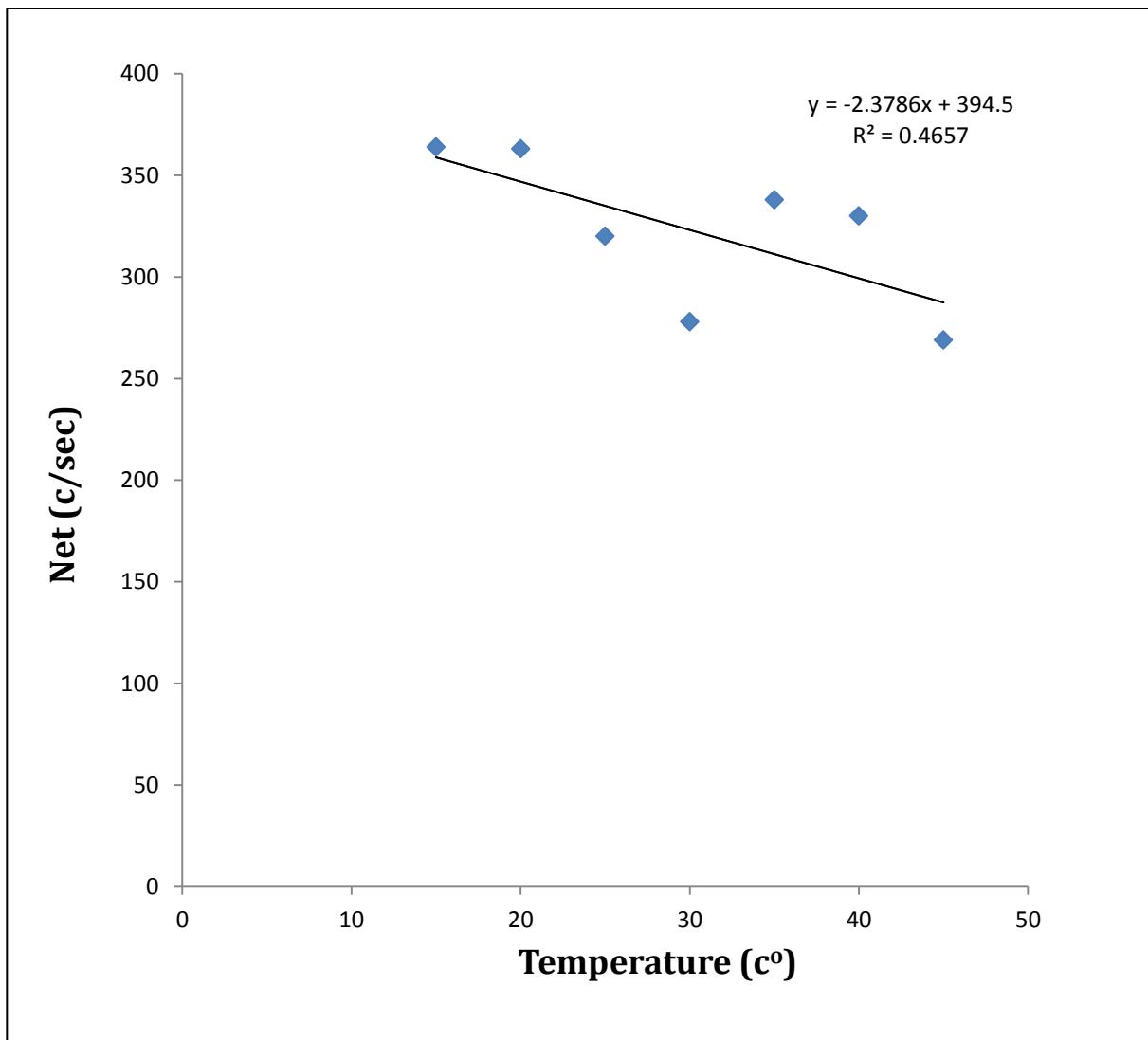


Figure (4.20) Distribution the net with change temperature for(Co-60) Total area.

From figure (4.20), the general behavior the net count decrease when temperature increases due the gamma photons decrease for total spectrum as a result of decrease in their interaction energy with increase in temperature and that is disagreement with previous study [40].

Study the effect of temperature on the gross for total area to the Co-60. The effect of temperature on the gross of the Co-60 spectrum and according to the results mentioned in Table (4.4), the relation between the change in the temperature and gross is drawn as shown in figure (4.21).

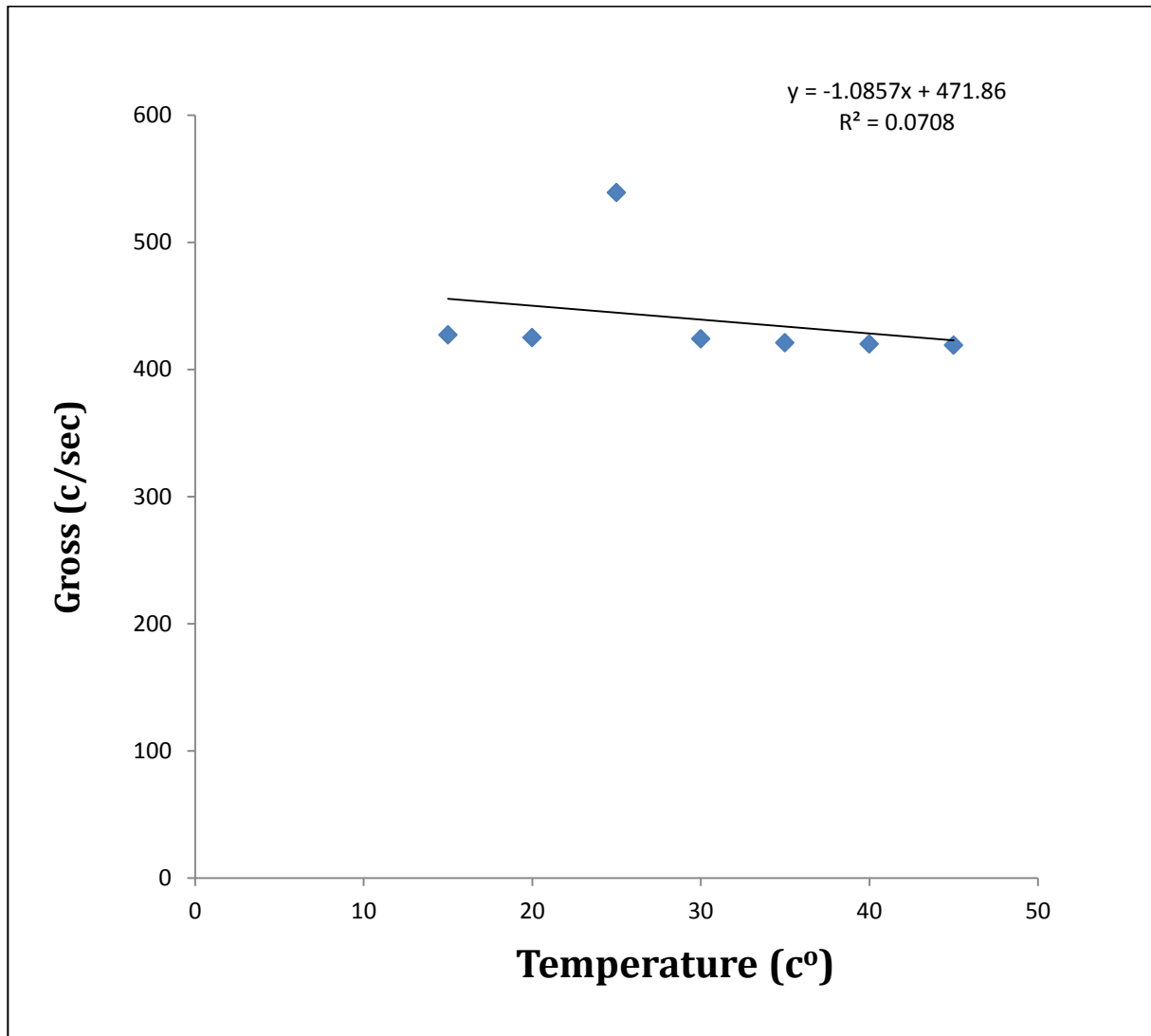


Figure (4.21) Distribution the gross with change temperature for (Co-60) Total area.

From figure (4.21), the general behavior the gross count decrease when temperature increases (inverse proportionality) due the gamma photons decrease for gross total spectrum as a result of decrease in their interaction energy with increase in temperature .

4.3.2 Photo Peak 1 at (1.173 MeV)

Study the effect (T) on the net photo peak 1 for Co-60. The effect of temperature on the net of the Co-60 spectrum and according to the results mentioned in Table (4.4), the relationship between the change in the temperature and net as shown in figure(4.22).

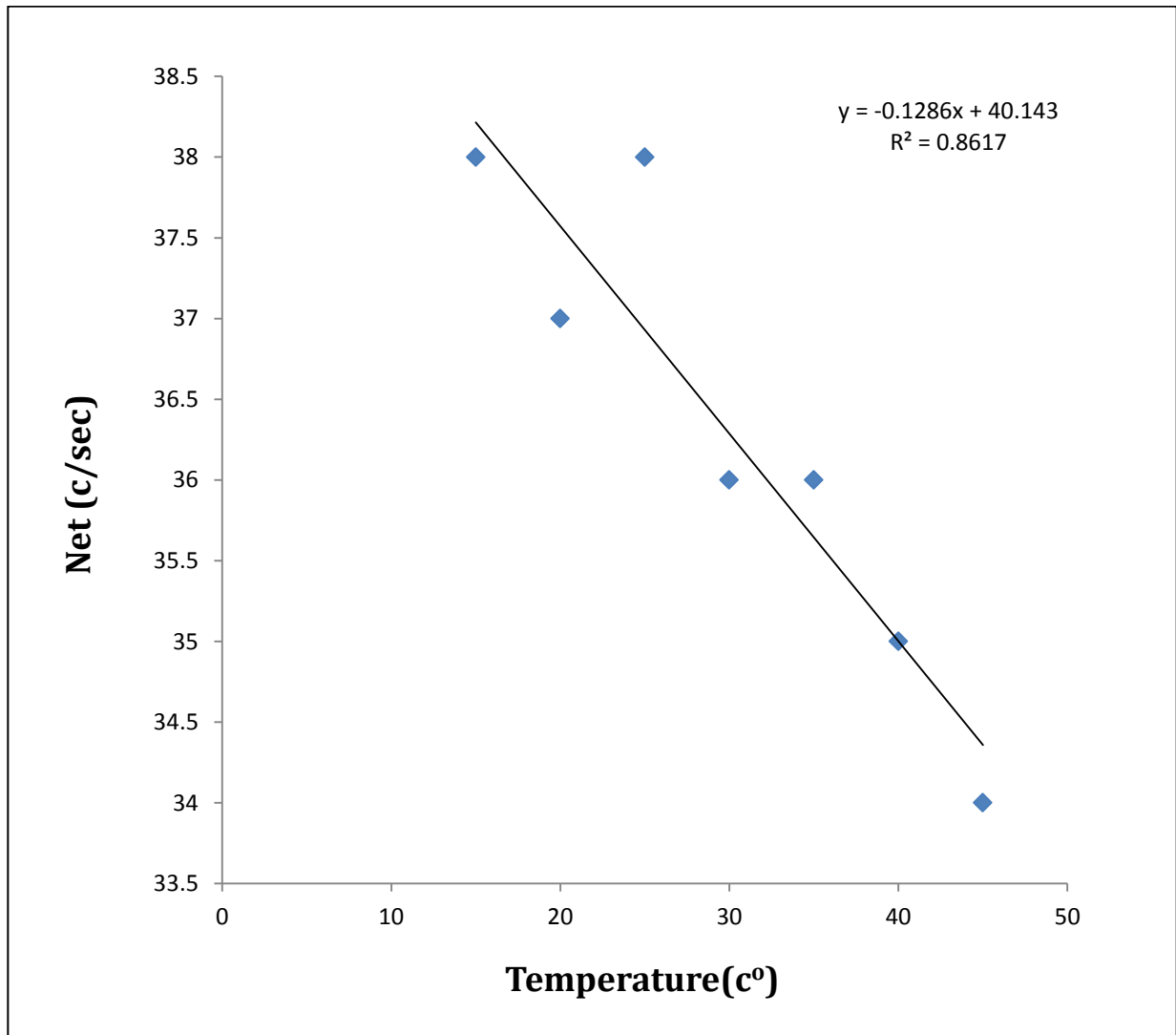


Figure (4.22) Distribution the net with change temperature for (Co-60) in the photo peak1.

From figure (4.22) the general behavior the net count decrease when temperature increases due the photons have back scattering with materials out detector for net photo peak1 when temperature increase and that is disagreement with previous study [40].

Study the effect of temperature on the gross for photo peak 1 to the Co-60. The effect of temperature on the gross of the Co-60 spectrum and according to the results mentioned in Table (4.4), the relation between the change in the temperature and gross as shown in figure (4.23).

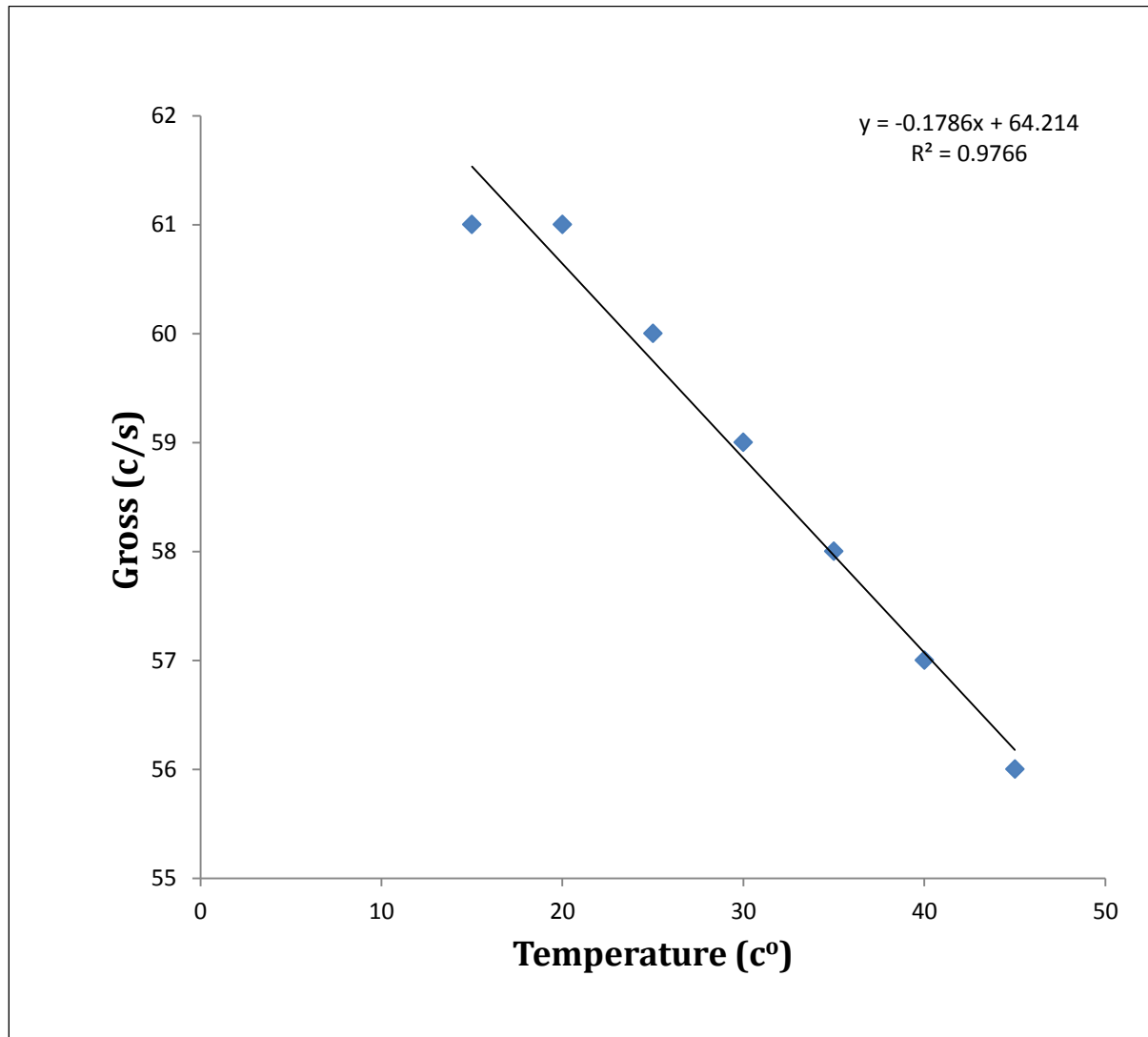


Figure (4.23) Distribute the gross with change temperature for (Co-60) photo peak1.

From figure (4.23), the general behavior the gross count decrease when temperature increases due the photons have back scattering with materials out detector for net photo peak1 when temperature increase and that is disagreement with previous study [40].

Study the effect of temperature on the full width of high maximum for photo peak 1 to the Co-60. The effect of temperature on the FWHM of the Co-60 spectrum and according to the results mentioned in Table (4.4), the relation between the change in the temperature and FWHM as shown in figure (4.24).

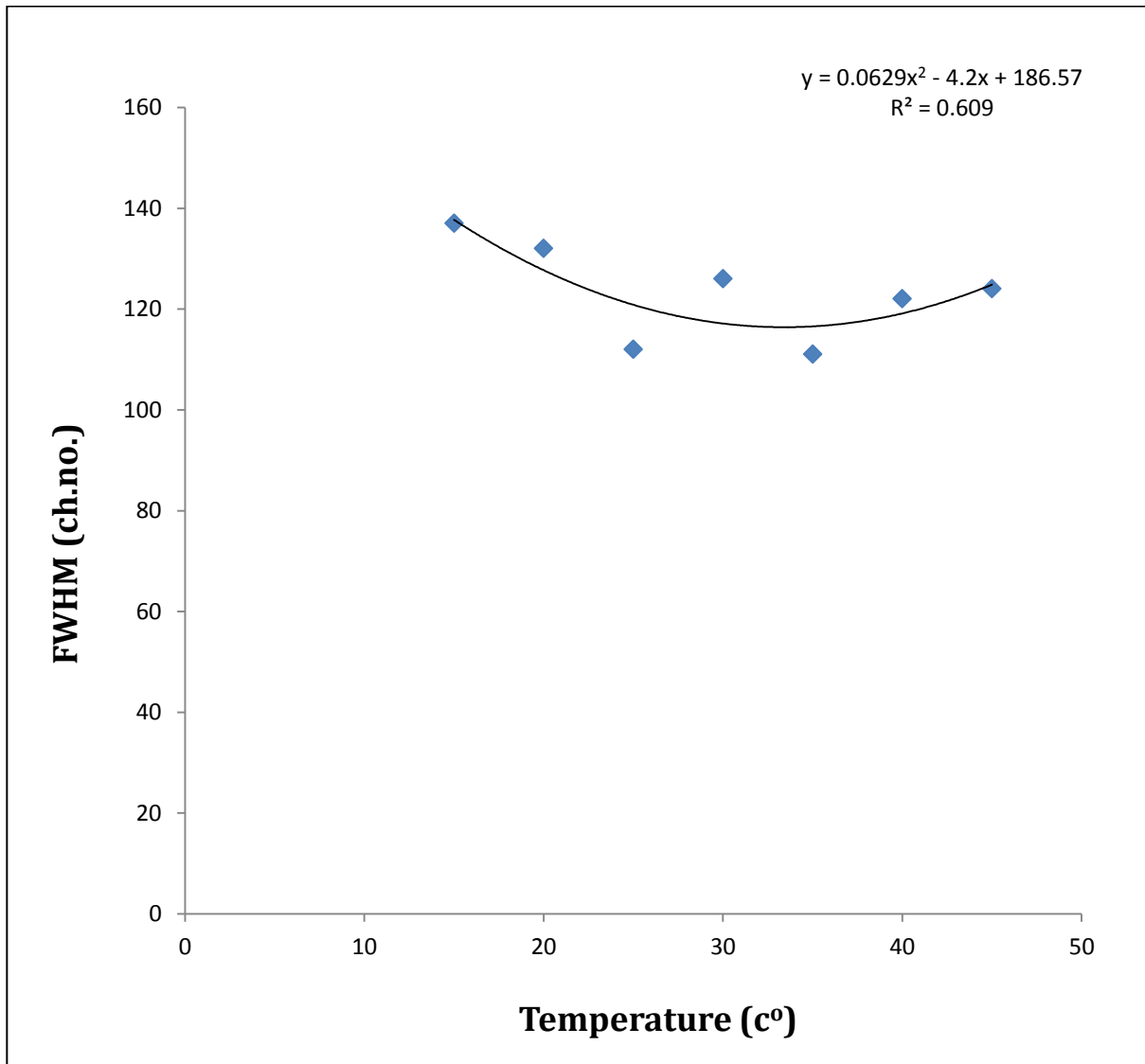


Figure (4.24) Distribution the FWHM with change temperature for (Co-60) photo peak1.

From figure (4.24), there is no clear behavior from the effect of temperature on FWHM for photo peak1 in Co-60 spectrum due of the unbalanced in the compression spectrum due the constant change in temperature .

The effect of temperature on the position photo peak1 for the Co-60. The effect of temperature on the centroid of the Co-60 spectrum and according to the results mentioned in Table (4.4), the relation between the change in the temperature and centroid as shown in figure (4.25). We note clearest graph showing between the temperature and the location of the light photo peak.

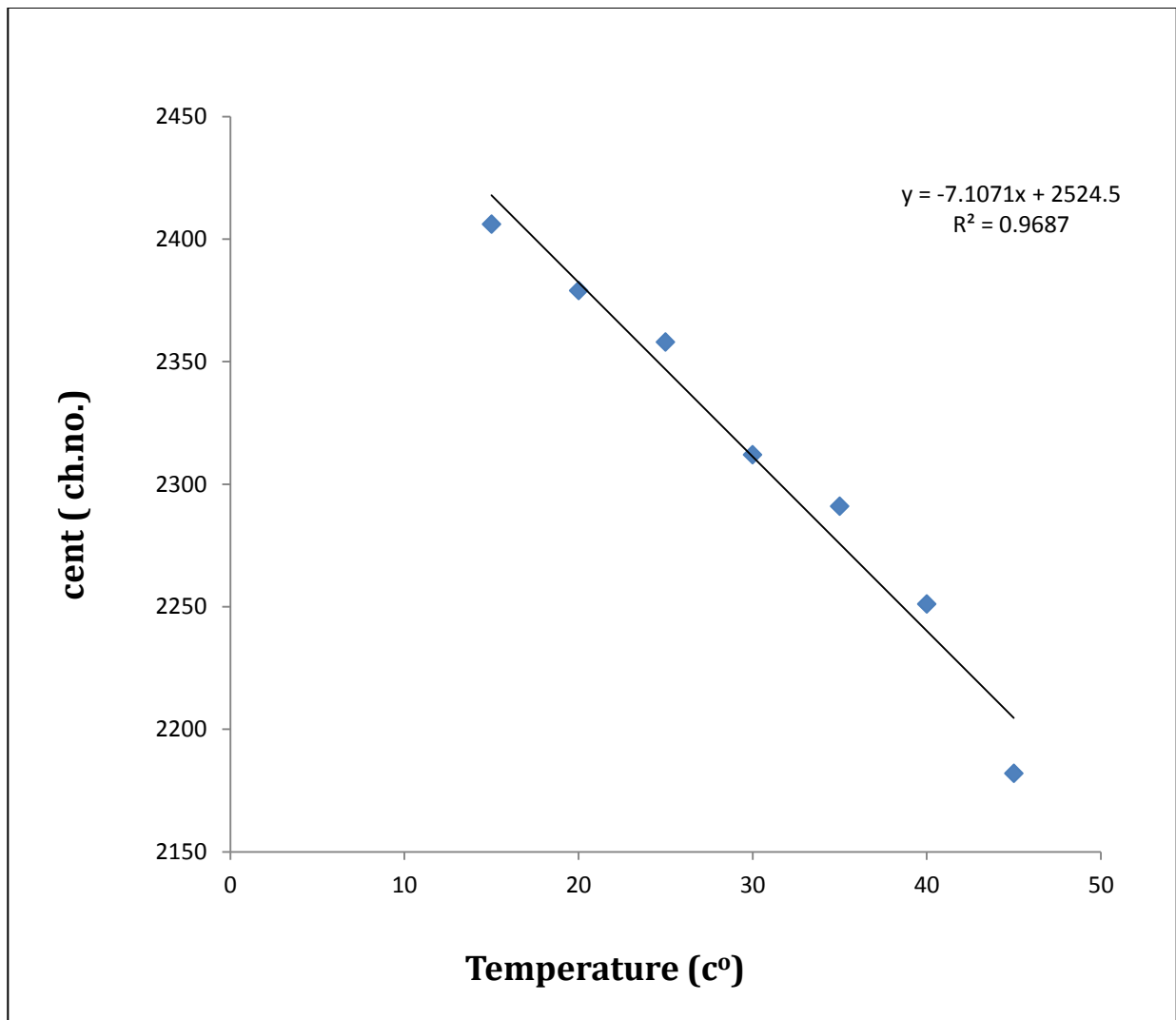


Figure (4.25) Distribution the position photo peak 1 with change temperature for (Co-60) photo peak1.

From figure (4.25) the relation between the temperature and position photo peak, we notice that there is an inverse proportionality, when temperature increases the centroid move to the lower energy levels. This agreed with previous study[40].

The effect (T) on the energy resolution (E.R) photo peak for the Co-60 spectrum .The results mentioned in Table (4.4), the relation between the change in the temperature and (E.R) is as shown in figure (4.26).

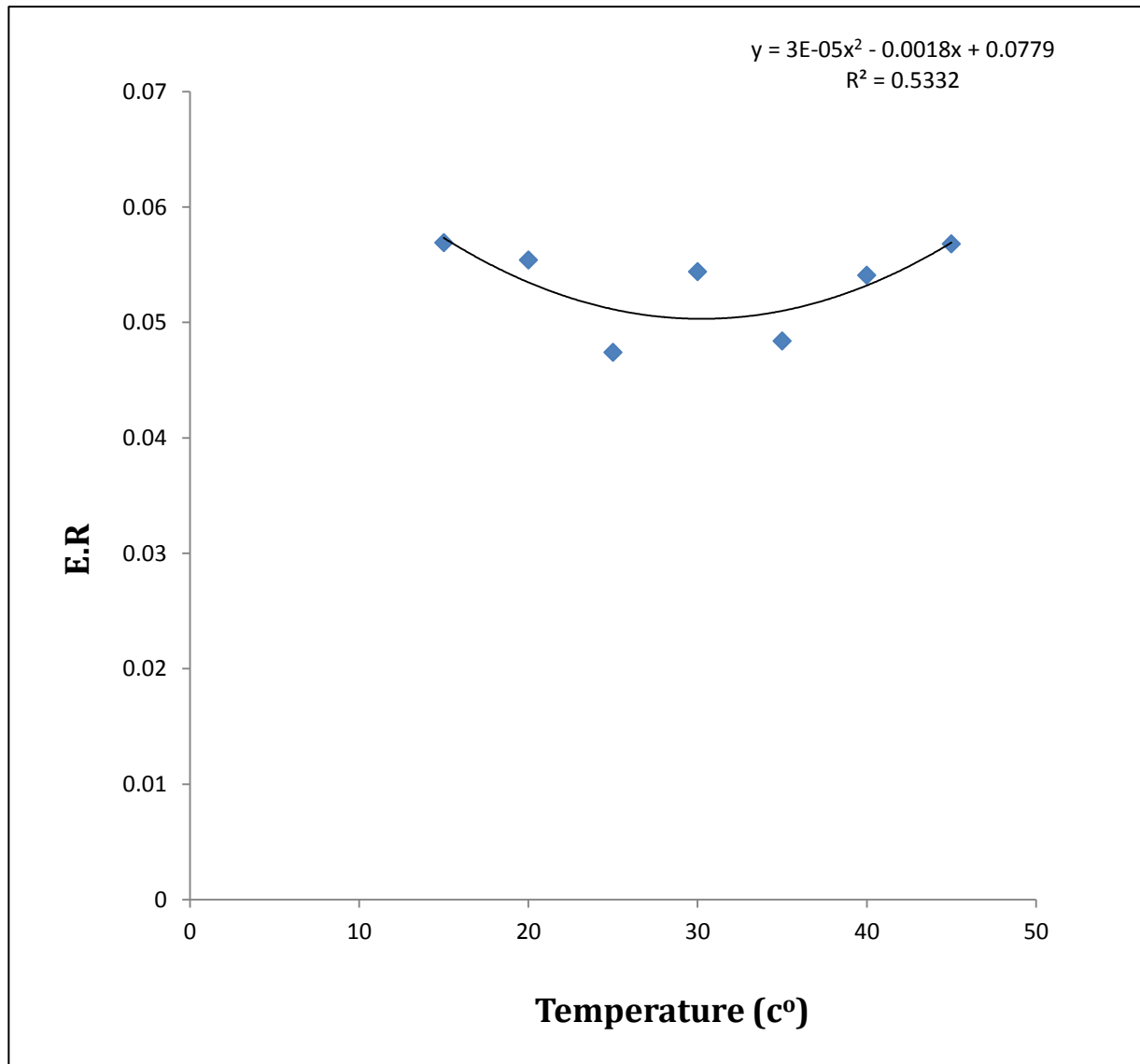


Figure (4.26) Distribution the E.R with change temperature for (Co-60) photo peak1.

From figure (4.26),found that the relationship between the E.R and temperature has no clear behavior (incomprehensible behavior) that is return to the change in the alternation (difference) of the FWHM values.

4.3.3 Photo Peak 2 at (1.332 MeV)

The effect of temperature on the second photo peak of cobalt Co- 60 was studied, and these results are shown in Table (4.5).

Table (4.5) the results of the effect of temperature on the second photo peak for (Co-60).

Temperature	Photo peak2 (1.332 MeV)				
T (c°)	Net (c/sec)	Gross (c/sec)	FWHM (ch.no.)	centroid (ch.no.)	E. R
15	36±6	47±7	135	2610	0.0517
20	33±6	46±7	143	2584	0.0553
25	32±6	46±7	135	2576	0.0524
30	31±6	45±7	122	2555	0.0477
35	31±6	44±7	139	2518	0.0552
40	30±5	43±7	116	2474	0.0468
45	29±5	43±7	120	2405	0.0498

Table (4.5) show the results obtained from effect temperature change on the area photo peak1 for the radioactive element (Co-60) in addition to the standard deviation.

The effect of (T) on the net photo peak2 for the Co-60 spectrum. According to the results mentioned in Table (4.5), the relation between the change in the temperature and net is drawn as shown in figure (4.27).

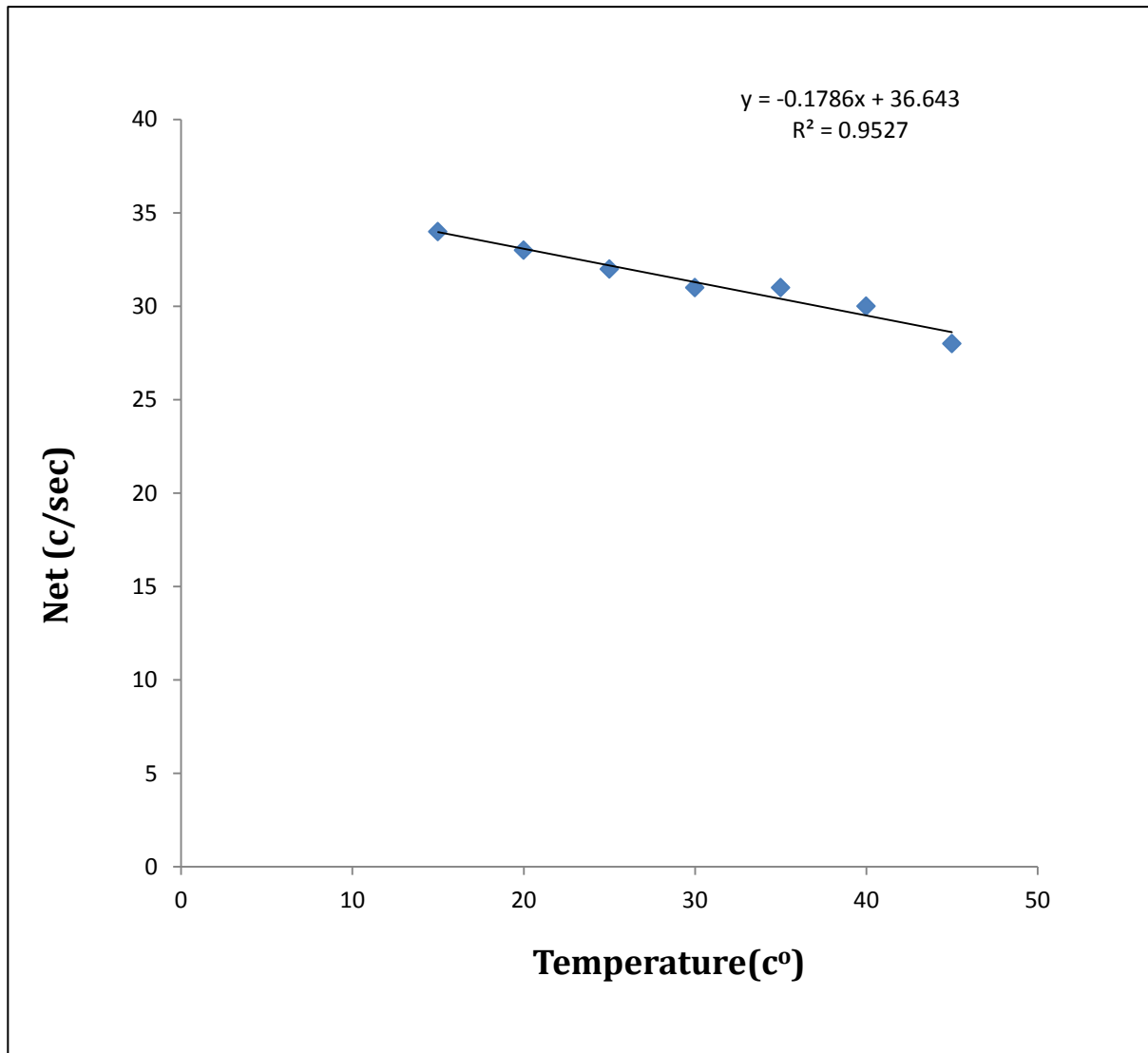


Figure (4.27) Distribution the net with change temperature for (Co-60) photo peak2.

From figure (4.27) found that the relationship between the net and temperature has inverse proportionality, due decrease in the energy of photons incident to the detector in the net photo peak2 and also because increase to the back scattering and this better from previous study [40].

The effect (T) on the gross photopeak2 for the Co-60 spectrum the effect of temperature on the gross of the (Co-60) spectrum and according to the results mentioned in Table (4.5), the relationship between the change in the temperature and gross as shown in figure (4.28).

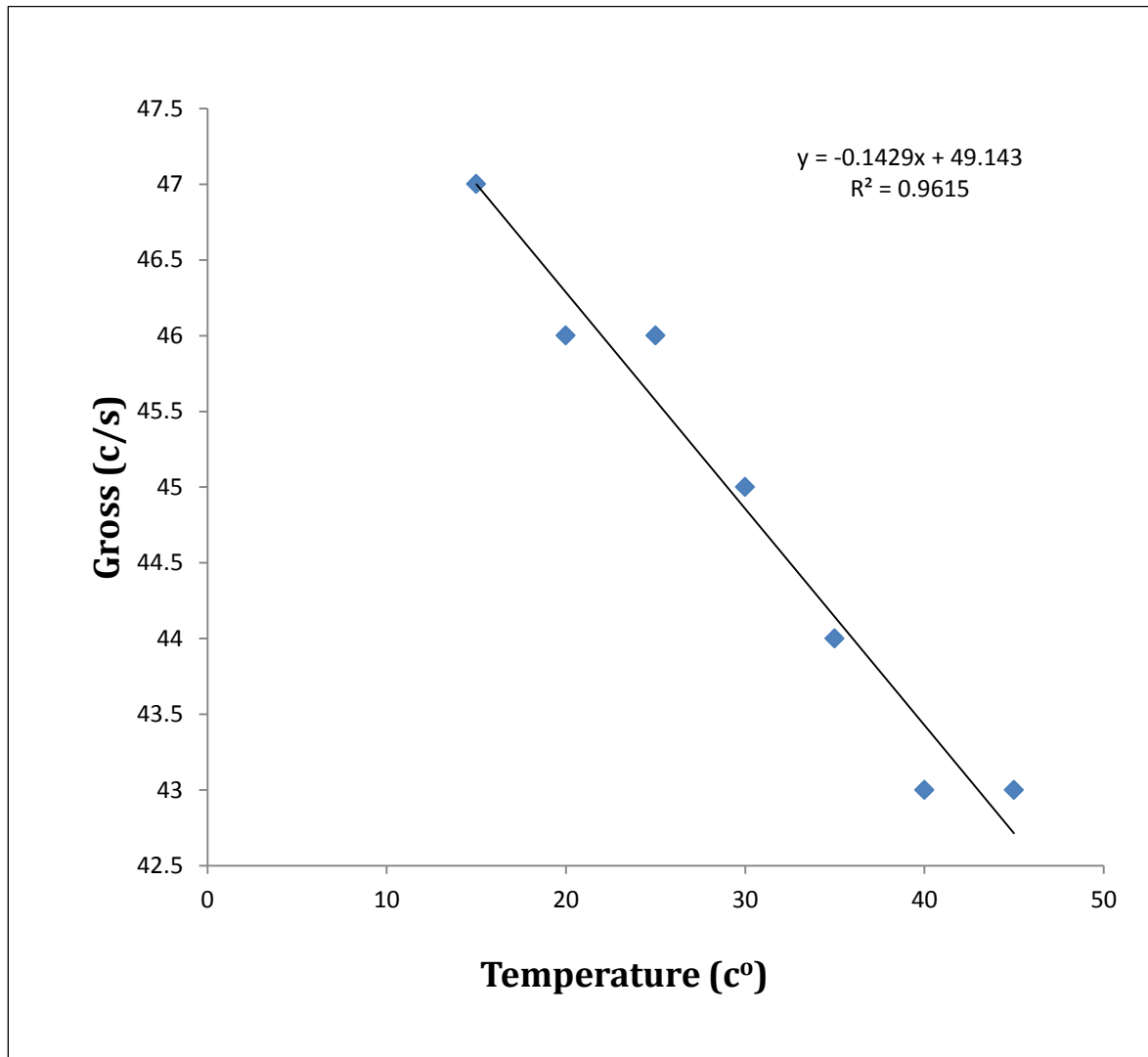


Figure (4.28) Distribution the gross with change temperature for (Co-60) photo peak2.

From figure (4.28) found that the relationship between the gross and temperature has inverse proportionality, due decrease in the energy of photons incident to the detector in the gross photo peak2 and also because increase to the back scattering and this better from previous study [40].

The effect temperature on the FWHM photopeak2 for the Co-60 spectrum, the effect of temperature on the FWHM of the Co-60 spectrum and according to the results mentioned in Table (4.5), the relation between the change in the temperature and FWHM as shown in figure (4.29).

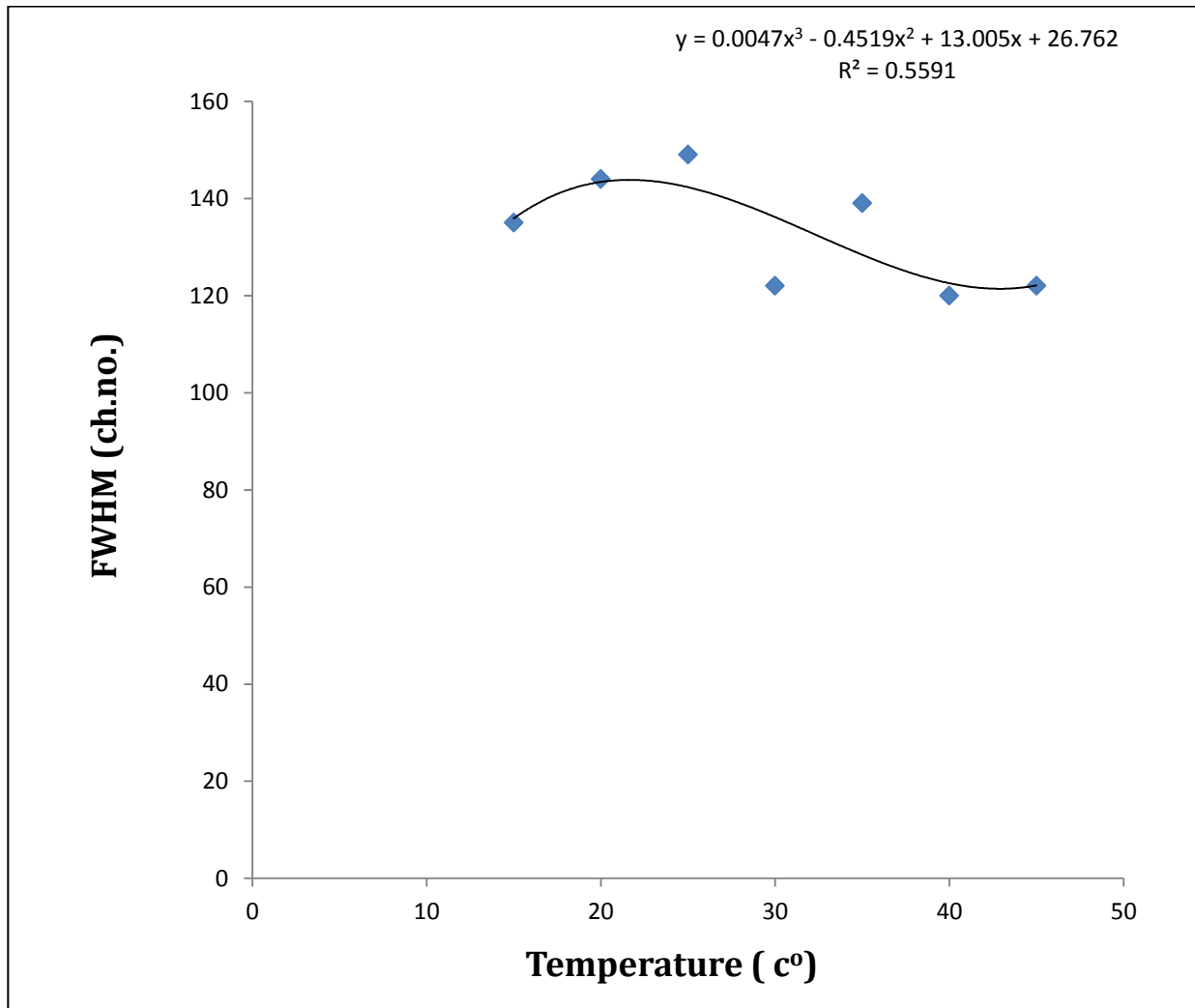


Figure (4.29) Distribution FWHM with change temperature for (Co-60) photo peak2.

From figure (4.29) ,found that the relationship between the FWHM and temperature has no clear behavior (incomprehensible behavior) because of the unbalanced in the compression spectrum due the constant change in temperature .

The effect of temperature on the position photo peak2 for the Co-60 .The effect of temperature on the centroid of the Co-60 spectrum and according to the results mentioned in Table (4.5), the relation between the change in the temperature and centroid as shown in figure(4.30).

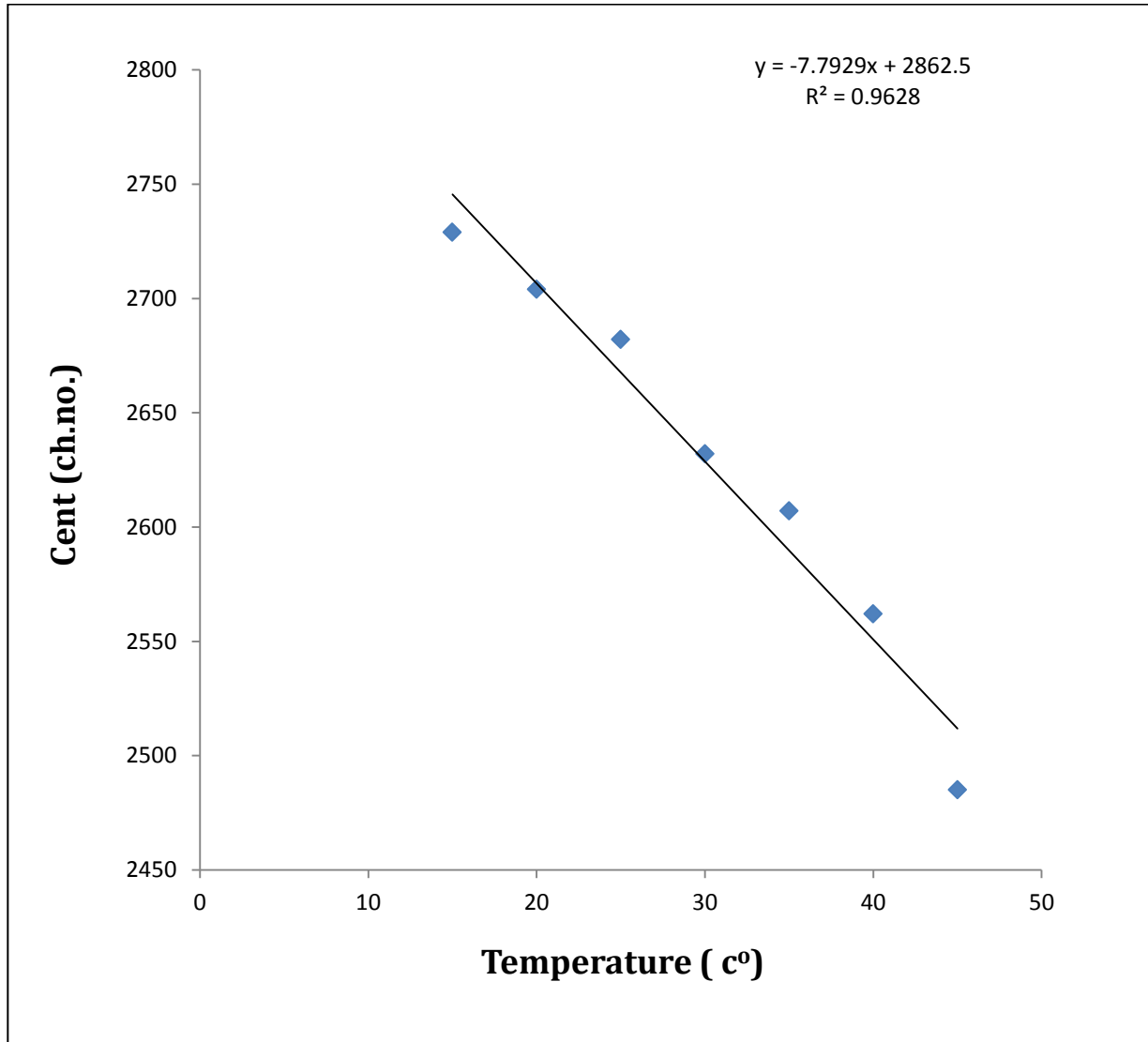


Figure (4.30) distribution the centroid with change temperature for (Co-60) photo peak2.

From figure (4.30), the relation between the temperature and position photo peak2, we notice that there is an inverse proportionality, the decrease in position photo peak is due influence of temperature factor and not from the radiation energy due compression the spectrum this agreed but better from previous study[40].

The influence of (T) on the energy resolution (E.R) photo peak2 for the Co-60 spectrum . According to the results mentioned in Table (4.5), the relation between the change in the temperature and (E.R) is drawn as shown in figure (4.31).

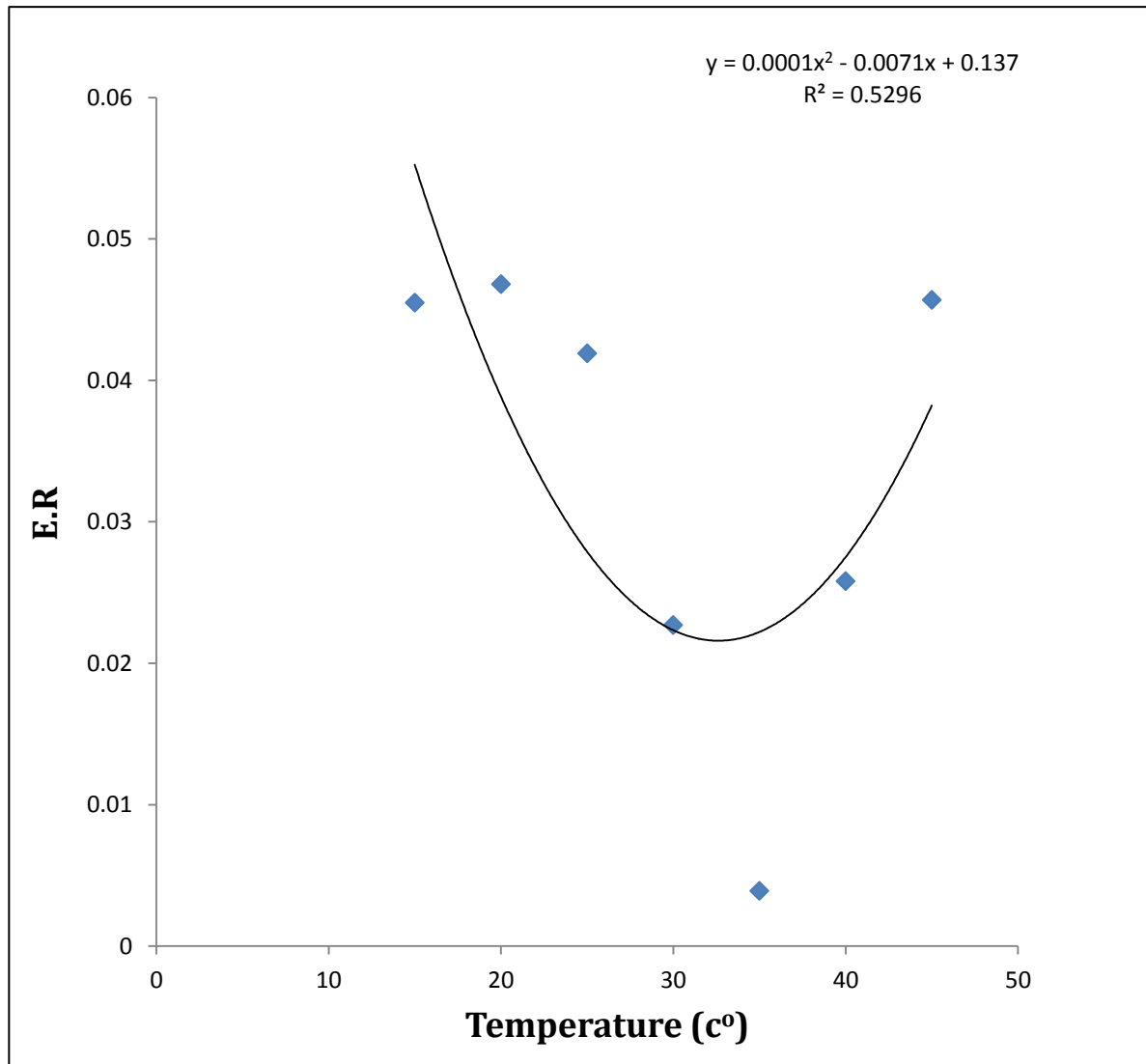


Figure (4.31) distribution the energy resolution with change temperature for (Co-60) photo peak2.

From figure (4.31), the relation between the E.R and temperature has no clear behavior (incomprehensible behavior) due the E.R dependence on the ratio between FWHM and centroid.

4.4 Conclusions

From the results obtained from three sources radioactive for gamma rays Cs-137, Na-22 and Co-60 at time constant 1000 sec can be concluded that.

1- The position of the photo peak (centroid) for total area , photo peak1 and photo peak2 for (Cs-137, Na-22 and Co-60) changes towards lower channels levels . This change is linear with an increasing in temperature from (15-45) C°.

2- The photo peak position move to the lower channel position due increases in temperature means a decrease in the amplitude of the electronic pulse resulting from the electronic counting system .

3- The effect of temperature on the (net and gross) for total spectrum area of radioactive sources (Cs-137, Na-22, Co-60) .It was found that in the spectrum for Cs-137 and Co-60 decreases with increasing temperature, but in the Na-22 spectrum increase when due used cooling instead heating.

4- The photo peak1 (net and gross) area of the radioactive sources (Cs-137, Na-22 and Co-60) was notice that the general behavior between (net and gross) and temperature inverse proportionality and FWHM for Cs-137 inverse proportionality but to Na-22 and Co-60 not have a clear behavior with increase in temperature.

5- In photo peak2 has same behavior a photo peak1 for all spectrums producing from all radioactive elements use in the experimental part.

6- It was found from this study, must be temperature stability to preservation of the environment at a certain temperature during use.

4.5 Future Works

- 1- Studying the effect of temperature on other types of detectors such as (HPGe).
- 2- Expansion of the study for the purpose of obtaining more information .Information that explains the behavior of some curves with random behavior (unclear behavior).

References

References

- [1]- G. Knoll, "Radiation Detection and Measurement", John Willey & Sons, New York ,2nd Ed,(2000).
- [2]- C. J. Martin, and D. G. Sutton,"Practical radiation protection in healthcare", Oxford University Press, USA. (Eds.) ,(2015).
- [3]- I. Akkurt, S. Kadir, S. Gunoglu, "Guidelines for limiting exposure in time-varying electric,magnatic and electromagnetic fields up to 300GHz",Health Physics,Vol.74,pp.494-522,(1998).
- [4]- T. Huang, Q. Fu, S. Lin, B. Wang, "NaI (Tl) scintillator read out with SiPM array for gamma spectrometer",Nuclear Instruments and Methods in Physics Research Section Accelerators, Spectrometers, Detectors and Associated Equipment,Vol.851,pp.118-124,(2017).
- [5]- H. Seo, C. H. Kim, J. H. Park, J. K. Kim, J. H. Lee, C. S. Lee, S. M. Kim and J. S. Lee,"Multitracing Capability of Double Scattering Compton Imager With NaI(Tl) Scintillator Absorber", IEEE,Vol. 57, No. 3, PP. 1420-1425,(2010).
- [6]- I. Rittersdorf, "Gamma Ray Spectroscopy", Nuclear Engineering and Radiological Scie ,pp.18-20,(2007).
- [7]- M. F. Annunziata , " Radioactivity Analysis" , Academic press ,New York, 2nd Ed, California,(2003).
- [8]- H.J. Arnikra , "Essentials of nuclear chemistry", 4th Ed ,New Age International (p), Ltd, (2005).
- [9]- P.L. Reeder and D. C. Stromswold, " Performance of Large NaI(Tl) Gamma-Ray Detectors Over Temperature(-50 to+60) Pacific Northwest National Laboratory", Richland, Washington ,(2004).
- [10]- A. A. Mowlavi, R.I. Najafbad and R. K. Faygh," Calculation of Intrinsic Efficiency of Detector Using MCNP Code", International Journal of Pure and Applied Physics NaI(Tl), Vol.1,pp.129-136,(2005).
- [11]- M. Nikl, "Scintillation detectors for x-rays", Measurement science and technology,Vol.17,p.37,(2006).

References

- [12]- N. Mercier, C. Falgueres, "Field gamma dose-rate measurement with a NaI (Tl) detector: re-evaluation of the threshold technique", journal *Ancient TL*, Vol.25, No.1, pp.1-4, (2007).
- [13]- A. D. Sabharwal , M. Singh, B. Singh and B. S. Sandhu, " Response Function of NaI(Tl) Detectors and multi backscattering of Gamma Rays in Aluminum", *Application. Radiation. Isotopes*, Vol.66, pp.1467-1473, (2008).
- [14]- K.D. Ianakiev, B.S. Alexandrov, P.B. Littlewood, M.C. Browne, "Temperature behavior of NaI (Tl) scintillation detectors". *Nuclear Instruments and Methods in Physics Research Section A: Accelerators, Spectrometers, Detectors and Associated Equipment*, Vol. 607, No.2, pp. 432-438, (2009).
- [15]- Y. Zhang, B. Wu, Y. Li, "Interior temperature monitoring of NaI(Tl) crystal in space environment by pulse width measurement", *Nuclear instrument and methods in physics research*, Vol.615, pp.272-276, (2010).
- [16]- N. C. Diaz, A. M. Sanchez, & J. de la Torre Perez, "SOLANG: A user-friendly code to calculate the geometry factor using Monte Carlo simulations: Application to alpha-particle spectrometry", *Applied Radiation and Isotopes*, Vol.6, No. 5, pp.822-824. (2011).
- [17]- C. Sailer, B. Lubsandorzhev, C. Strandhagen, J. Jochum, "Low temperature light yield measurements in NaI and NaI (Tl)", *The European Physical Journal*, Vol 72, No.6, pp.1-4, (2012).
- [18]- M. A. Elzaher¹, M.S. Badawi, A. El-Khatib and Abo. Ahmed Thabet, "Determination of Full Energy Peak Efficiency of NaI(Tl) Detector Depending on Efficiency Transfer Principle for", *World Journal of Nuclear Science and Technology*, Vol.2, pp.65-72, (2012).
- [19]- B. Oto, A. Gur, M. R. Kacal, B. Dogan, " Photon attenuation properties of some concretes containing barite and colemanite in different rates", *Annals of Nuclear energy*, Vol. 51, pp. 120-124, (2013).
- [20]- A. Simon, S. J. Quinn, A. Spyrou, A. Battaglia, I. Beskin, A. Best, M. Wiescher, " SuN: Summing NaI (Tl) gamma-ray detector for capture reaction measurements",

References

Nuclear Instruments and Methods in Physics Research Section A: Accelerators, Spectrometers, Detectors and Associated Equipment, Vol.703,pp.16-21. (2013).

[21]- K. U. Kiran, K. Ravindraswami, K.M. Eshwarappa , H.M Somashekarap, "An investigation of energy dependence on saturation thickness for 59.54, 123, 279, 360, 511, 662,1115 and 1250 KeV gamma photons in carbon and aluminum", Radiation Physics and Chemistry, Vol.97,pp.107-112,(2014).

[22]- S. Takeuchi,T. Motobayashi, Y. Togano, M. Matsushita, N. Aoi, K. Demichi, H. Hasegawa, H. Murakami, "DALI2: A NaI (Tl) detector array for measurements of γ rays from fast nuclei", Nuclear Instruments and Methods in Physics Research Section A: Accelerators, Spectrometers, Detectors and Associated Equipment, Vol. 763,pp.596-603,(2014).

[23]- Y. Liu,Y. Zhang , C. Li, D. Liu, "Monte Carlo simulation of a NaI (Tl) detector for in situ radioactivity measurements in the marine environment", Applied Radiation and Isotopes, Vol.98,pp.44-48,(2015).

[24]- P. Mitra, A.S. Roy, A. K. Verma, A.D. Pant, M.S. Prakasha,S. Anilkumar, and A.V. Kumar,"Application of spectrum shifting methodology to restore NaI (Tl)-recorded gamma spectra, shifted due to temperature variations in the environment", Applied Radiation and Isotopes,Vol.107,pp.133-137,(2016).

[25]- D. Souza, E. Barbosa, J. Cherwinka, A. Cole, A.C. Ezeribe, D. Grant, F. Halzen, K.M. Heeger, L. Hsu, A. Hubbard, J. Jo, A. Karle, M. Kauer, VA. Kudryavtsev, KE. Lim, C. Macdonald, RH. Maruyama, F. Mouton, SM. Paling, W Pettus, ZP. Pierpoint, BN. Reilly, M. Robinson, FR. Rogers, P. Sandstrom, A. Scarff, NJC. Spooner,S. Telfer, L. Yang,DM-Ice Collaboration,"First search for a dark matter annual modulation signal with NaI (Tl) in the Southern Hemisphere by DM-Ice17", Physical Review,Vol.95,P.3206,(2017).

[26]- L. E. C. Robalino, G. F. G. Fernandez, E. Gallego,K. A. Guzman-Garcia, H. R. Vega-Carrillo, " Study by Monte Carlo methods of an explosives detection system made up with a DD neutron generator and NaI (Tl) gamma detectors", Applied Radiation and Isotopes,Vol.141,pp.167-175,(2018).

References

- [27]- M. K. Bakhshayesh, "Development of an efficient technique for constructing energy spectrum of NaI (Tl) detector using spectrum of NE102 detector based on supervised model-free methods", *Radiation Physics and Chemistry*, Vol 176, p.1063, (2020).
- [28]- R. S. Ahmed. "A review on soil radionuclide distribution in Iraq analysed using gamma ray spectroscopy", *Environmental Forensics*, Vol.22, pp.91-98, (2021).
- [29]- L.J. Bignell, I. Mahmood, F. Nuti, G. J. Lane, A. Akber, E. Barberio , M. Zurowski, "Quenching factor measurements of sodium nuclear recoils in NaI: Tl determined by spectrum fitting", *journal instrumentation*, Vol.16, p.7034, (2021).
- [30]- P. A. Amado, V. A. Amado and J. C. Aguiar, "Full-energy pea determination from total efficiency and peak to total ratio calculations" *Nuclear Instrument and methods in physics research A*, Vol.990, pp.1-15, (2021).
- [31]- F.M. Khan and J.P. Gibbons, "Khan's the physics of radiation therapy" *Lippincott Williams & Wilkins*, (2014).
- [32]- O.N. Ottawa, "Minister of Public Work and Government Services. Government of Canada", (2015).
- [33]- M.F. L Annunziata, "Radioactivity Analysis", *Academic press*, New York 2nd Ed., Californi, (2003).
- [34]- P.H. Hendriks, J. Limburg, R.J. De Meijer, "Full-spectrum analysis of natural γ -ray spectra", *Journal of Environmental Radioactivity*, Vol.53, pp.365-380, (2001).
- [35]- N. Tsoulfanidis, "Measurement and Detection of Radiation", 2nd Ed., *Taylor and Francis*, Washington DC, (1995).
- [36]- G. Knoll, "Nuclear and Particle Physics", *John Wiley : U.S.A*, 3rd Ed, (2006).
- [37]- H. Youn Cho, J.U. Hahn Lee, C.S. Lee, "Improvement of Time Resolution of BaF₂ Scintillator for Low – Energy Gamma Rays by Digital Pulse – Shape Method", *IEEE*, Vol.57, PP.1386-1390, (2010).
- [38]- J.S. Blackmore, "Solid State Physics", *Gambridge Press*, 2nd Ed, (1986).

References

- [39]- W.M. Hibbard , "Effects of Temperature Changes on NaI Crystals", Journal of Nuclear Medicine Technology, Vol.3, pp.168-169, (1975).
- [40]- A.H. Khalid, "The factors affecting the response function of the scintillation detector NaI(Tl)", Master Thesis University of Baghdad ,(1988).
- [41]- W. Xu, H. Xu, S. H. Wang, Z. Wang, X. Xu, X. Zhang, S. Wu, "Scintillation materials based on metal iodates by rare earth doping modifications for use in radio luminescence and X-ray imaging", Crystal Engineering Comm, Vol.23, pp.4103-4108, (2021).
- [42]- G. Knoll, "Radiation detection and Measurement ", John Wiley & Sons , New York, 4th Ed, (2010).
- [43]- C. Lee, W. S. Sul, H. Kim, C. Kim, G. Cho, "Effect on MIM structured parallel quenching capacitor of SiPMs", Nuclear Instruments and Methods in Physics Research Section A: Accelerators, Spectrometers, Detectors and Associated Equipment, Vol.650, pp.125-128, (2011).
- [44]- G. Cho, H. Kim, W. S. Sul, C. Lee, B. S. Kang, "Optimum design of quenching capacitor integrated silicon photomultipliers for TOF-PET application", Physics Procedia, Vol.37, pp.1511-1517, (2012).
- [45]- M. Bondi, M. Battaglieri, M. Carpinelli, A. Celentano , M. De Napoli, R. De Vita, L. Marsicano, N. Randazzo, V. Sipala, E.S. Smith, " large-size CsI(Tl) Crystal read- out by SiPM for low-energy charged –particles detection ", Nucl. Instrum. Methods, Vol.867, pp.148-153, (2017).
- [46]- J. Culver, W .Akers, S. Achilefu, "Multimodality molecular imaging with combined optical and SPECT/PET modalities", J Nucl Med, Vol.49, pp.169–72, (2008).
- [47]- EV. Garcia, TL. Faber, FP. Esteves, "Cardiac dedicated ultrafast SPECT cameras: New designs and clinical implications", Journal Nuclear Medicine, Vol.52, pp.210–217, (2011).
- [48]- A. Rahmim, H. Zaidi, "PET versus SPECT: Strengths, limitations and challenges", Nuclear Medicine Community, Vol.29, pp.193–207, (2008).

References

- [49]- M. Khoshakhlagh, J. P. Abedi, S. M. Mahmoudian, "Development of scintillators in nuclear medicine", World journal of nuclear medicine, Vol.14, No.3, p.156, (2015).
- [50]- Mkt-intl.com. "Scintillation crystal material", Available from: Last updated on Apr 03, (2014).
- [51]- M.A. Fida, F. Liu, M. Li, T. Jiang, X. Fan, "Response Function Simulation of Labr3 (Ce) Scintillation Detector", Journal of Physics: Conference Series, Vol. 1739, No.1, p.1202, (2021).
- [52]- Gamma-rays spectroscopy using NaI(Tl), Experiments in Nuclear Science Laboratory Manual, ORTEC, 4th Ed, (2014).
- [53]- E.F Giraldo, A.A. Ruales, L.F Ramirez, J.E. Tobon, J.H Lopez, C.A. Barrero, "Open the multichannel analyzer and remote monitor for Mossbauer spectroscopy", Hyperfine interactions, Vol.241, No.1, pp.1-9, (2020).
- [54]- C. W. E. Eijk, "Inorganic-scintillator Development", Nuclear. Instrument. Methods Physics. Res Section, Vol.460, pp.1-14, (2001).

الخلاصة

تم دراسة تأثير درجة حرارة الجو على طيف الطاقة بواسطة كاشف الومبيضي في هذا العمل . تم استخدام عدة مصادر قياسية للنظائر المشعة التالية السيزيوم (Cs -137) , الصوديوم (Na -22) , الكوبالت (Co-60) تم استخدام مصدر حرارة للتحكم بدرجة الحرارة و تم استخدام محارير على الجانب الايمن والايسر من الكاشف لقياس درجة الحرارة المناسبة . استخدمت حاوية مع غطاء عازل للحرارة تغطي كل هذه الاجزاء التي تم استخدامها في الجانب العملي لكي تبقى درجة الحرارة ثابتة للحصول على افضل النتائج.

وقد وجد انه موقع القمة الضوئية يتناقص في مساحة الطيف مع ازدياد درجة الحرارة في اطيف كل العناصر المشعة التي تم استخدامها وهو افضل وواضح سلوك تم الحصول عليه، اما بقية النتائج للمساحات الاخرى في بعض الاحيان يكون تأثيرها مع ازدياد درجة الحرارة تمتاز بان لها سلوك غير واضح.

من خلال النتائج التي تم الحصول عليها وجد ان موقع القمة الضوئية للطيف الناتج تتأثر بدرجات الحرارة اي كلما تزداد درجة الحرارة ينضغط الطيف الناتج من كاشف الومبيضي وموقع القمة يزحف نحو مستويات الطاقة الاوطأ من، لذا يجب ان تكون درجة الحرارة ثابتة عند الاستخدام.



جمهورية العراق

وزارة التعليم العالي والبحث العلمي

كلية العلوم / جامعة بابل

قسم الفيزياء

دراسة تأثير درجة حرارة الجو على اطياف اشعة كاما

للكاشف الوميضي NaI(Tl)

رسالة مقدمة الى

مجلس كلية العلوم - جامعة بابل

وهي جزء من متطلبات نيل درجة الماجستير في العلوم / الفيزياء

من قبل

عباس حسن عبدالله زعيري

بإشراف

أ.د. خالد حسين هاتف العطية